J|A|C|S
ARTICLES
Published on Web 03/23/2007

Alkylthio Bridged 44 cve Triangular Platinum Clusters: Synthesis, Oxidation, Degradation, Ligand Substitution, and Quantum Chemical Calculations

Christian Albrecht,[†] Sebastian Schwieger,[†] Clemens Bruhn,[‡] Christoph Wagner,[†] Ralph Kluge,[†] Harry Schmidt,[†] and Dirk Steinborn*[,†]

Contribution from the Institut für Anorganische Chemie, Martin-Luther-Universität Halle-Wittenberg, Kurt-Mothes-Straβe 2, D-06120 Halle, Germany, and Institut für Chemie, Universität Kassel, Heinrich-Plett-Straβe 40, D-34132 Kassel, Germany

Received November 27, 2006; E-mail: steinborn@chemie.uni-halle.de

Abstract: Acetylplatinum(II) complexes *trans*-[Pt(COMe)Cl(L)$_2$] (L = PPh_3, **2a**; P(4-FC_6H_4)$_3$, **2b**) were found to react with dialkyldisulfides R_2S_2 (R = Me, Et, Pr, Bu; Pr = *n*-propyl, Bu = *n*-butyl), yielding trinuclear 44 cve (cluster valence electrons) platinum clusters [(PtL)$_3$(μ-SR)$_3$]Cl (**4**). The analogous reaction of **2a**−**b** with Ph_2S_2 gave SPh bridged dinuclear complexes *trans*-[{PtCl(L)}$_2$(μ-SPh)$_2$] (**5**), whereas the addition of Bn_2S_2 (Bn = benzyl) to **2a** ended up in the formation of [{Pt(PPh_3)}$_3$(μ_3-S)(μ-SBn)$_3$]Cl (**6**). Theoretical studies based on the AIM theory revealed that type **4** complexes must be regarded as triangular platinum clusters with Pt−Pt bonds whereas complex **6** must be treated as a sulfur capped 48 ve (valence electrons) trinuclear platinum(II) complex without Pt−Pt bonding interactions. Phosphine ligands with a lower donor capability in clusters **4** proved to be subject to substitution by stronger donating monodentate phosphine ligands (L′ = $PMePh_2$, PMe_2Ph, PBu_3) yielding clusters [(PtL′)$_3$(μ-SR)$_3$]Cl (**9**). In case of the reaction of clusters **4** and **9** with $PPh_2CH_2PPh_2$ (dppm), a fragmentation reaction occurred, and the complexes [(PtL)$_2$(μ-SMe)(μ-dppm)]Cl (**12**) and [Pt(μ-SMe)$_2$(dppm)] (**13**) were isolated. Furthermore, oxidation reactions of cluster [{Pt(PPh_3)}$_3$(μ-SMe)$_3$]Cl (**4a**) using halogens (Br_2, I_2) gave dimeric platinum(II) complexes *cis*-[{PtX(PPh_3)}$_2$(μ-SMe)$_2$] (**14**, X = Br, I) whereas oxidation reactions using sulfur and selenium afforded chalcogen capped trinuclear 48 ve complexes [{Pt(PPh_3)}$_3$(μ_3-E)(μ-SMe)$_3$] (**15**, E = S, Se). All compounds were fully characterized by means of NMR and IR spectroscopy, microanalyses, and ESI mass spectrometry. Furthermore, X-ray diffraction analyses were performed for the triangular cluster **4a**, the trinuclear complex **6**, as well as for the dinuclear complexes *trans*-[{Pt($AsPh_3$)}$_2$(μ-SPh)$_2$] (**5c**), [{Pt(PPh_3)}$_2$(μ-SMe)(μ-dppm)]Cl (**12a**), and [{{PtBr(PPh_3)}$_2$(μ-SMe)$_2$] (**14a**).

Introduction

The research of metal clusters is a recognizable discipline in the field of inorganic chemistry that gains continuously in importance because of the special electrical, magnetical, chemical, and especially catalytical properties of these compounds.[1] Over several decades, a plethora of large polyhedral clusters were synthesized that reach deep into the nano scale.[2] According to the definition of a metal cluster, "a finite group of metal atoms that are held together mainly or at least to a significant extent, by bonds directly between the metal atoms, even though some non-metal atoms may also be intimately associated with the cluster",[3] the triangular M_3 unit represents the smallest cluster of all. Furthermore, M_3 units can be regarded as the smallest section of metal surfaces or crystallites. This demonstrates that the chemistry of naked and ligand-stabilized electron variable M_3 clusters may build a bridge between molecular chemistry, solid-state chemistry, and nano science. Hence, the detailed research of the electronic situation and the structural variety of triangular clusters, especially of the late transition metal clusters, are of major and fundamental importance.

Triangular platinum clusters from 42 up to 46 cluster valence electrons (cve) have been prepared with the 42 cve clusters being the most prevalent ones. All of these clusters possess bridging ligands that may be μ_2 ligands like CO, SO_2, H, CNR as represented by [{Pt(PR_3)}$_3$(μ-CO)$_3$],[4] [{Pt(PR_3)}$_3$(μ-SO_2)$_3$],[5] [{PtH(PR_3)}$_3$(μ-H)$_3$],[6] and [{Pt(CNR)}$_3$(μ-CNR)$_3$],[7] bidentate ligands like bis(diphenylphosphino)methane (dppm) in [Pt_3(CNR)$_2$(μ-dppm)$_3$](PF_6)$_2$,[8] or μ_3 ligands like CO, H in [Pt_3Cl(μ_3-CO)(μ-dppm)$_3$]Cl,[9] and [{Pt(μ-dppm)}$_3$(μ_3-H)](PF_6).[10] Ob-

[†] Martin-Luther-Universität Halle-Wittenberg.
[‡] Universität Kassel.

(1) Moskovits, M. *Metal Clusters*; John Wiley & Sons: New York, 1986.
(2) Braunstein, P.; Oro, L. A.; Raithby, P. R. *Metal Clusters in Chemistry*; Wiley-VCH: Weinheim, 1999.
(3) Shriver, D. F.; Kaesz, H. D.; Adams, R. D. *The Chemistry of Metal Cluster Complexes*; VCH Publishers, Inc.: New York, 1990.
(4) Moor, A.; Pregosin, P. S.; Venanzi, L. M. *Inorg. Chim. Acta* **1981**, *48*, 153.
(5) Ros, R.; Tassan, A.; Laurenczy, G.; Roulet, R. *Inorg. Chim. Acta* **2000**, *303*, 94.
(6) Dahmen, K. H.; Imhof, D.; Venanzi, L. M. *Helv. Chim. Acta* **1994**, *77*, 1029.
(7) Haggit, J. L.; Mingos, D. M. P. *J. Organomet. Chem.* **1993**, *462*, 365.
(8) Bradford, A. M.; Payne, N. C.; Puddephatt, R. J.; Yang, D. S.; Marder, T. B. *J. Chem. Soc. Chem. Commun.* **1990**, 1462.

10.1021/ja068476r CCC: $37.00

viously, such bridging ligands are important for the stability, as has been demonstrated by quantum chemical calculations.[11] Furthermore, the presence of bridging ligands has consequences in terms of the symmetry. Whereas D_{3h} symmetry was found in most of the 42 cve triangular platinum clusters or, at least, in the cluster cores like in $[\{Pt(PR_3)\}_3(\mu\text{-}CO)_3]$, the electronic and steric effects of the bridging ligands in the 44 cve clusters, such as $[Pt_3(CNR)_2(\mu\text{-dppm})_3](PF_6)_2$[8] or $[Pt_3Cl(\mu_3\text{-}CO)(\mu\text{-dppm})_3]Cl$,[9] give rise to a wide variety of geometrical conformations and complex structures. Thus, higher symmetrical 44 cve triangular platinum clusters having C_{3v} or D_{3h} symmetry are relatively rare and all are cationic clusters containing bridging three electron donor μ-PR_2 ligands. Such clusters can be described with the simplified formula $[(PtL)_3(\mu\text{-}PR_2)_3]^+$ (L = PR_3, CO, CNR) or as 3:3:3-type clusters.[12,13] Noteworthy, up to now, no higher symmetrical triangular platinum cluster containing other bridging three electron donor ligands are known.

In this paper, we report the syntheses and spectroscopic and structural characterization of novel C_{3v} symmetrical 44 cve triangular platinum clusters $[(PtL)_3(\mu\text{-}SR)_3]Cl$ (**4**, L = PR_3, R = Me−Bu; **8**, L = $AsPh_3$, R = Me). Taking advantage of the robust nature of the Pt−S−Pt bridges,[14] the reactivity of these clusters toward halogens, chalcogens, and phosphines yielding dinuclear platinum(II) complexes *cis*-$[\{PtX(L)\}_2(\mu\text{-}SR)_2]$ (**14**, X = Br, I), trinuclear chalcogen capped platinum(II) complexes $[(PtL)_3(\mu_3\text{-}E)(\mu\text{-}SR)_3]Cl$ (**15**, E = S, Se), and dinuclear platinum(I) complexes $[(PtL)_2(\mu\text{-}SR)(\mu\text{-dppm})]Cl$ (**12**) will be discussed. Quantum chemical calculations were performed to gain a deeper understanding of the bonding models in such platinum clusters.

2. Results and Discussion

2.1. Reactivity of Acetylplatinum(II) Complexes toward Diorganodisulfides. We reported earlier that reactions of the dinuclear platina-β-diketone $[Pt_2\{(COMe)_2H\}_2(\mu\text{-}Cl)_2]$ (**1**) with phosphine and arsine ligands are very convenient routes for the preparation of acetylplatinum(II) complexes *trans*-$[PtCl(COMe)(L)_2]$ (**2**) (Scheme 1, path **a**).[15]

Acetylplatinum(II) complexes **2a**/**b** were found to react with an excess of dialkyldisulfides (Me_2S_2, Et_2S_2, Pr_2S_2, Bu_2S_2), yielding novel 44 cve cationic triangular platinum clusters $[(PtL)_3(\mu\text{-}SR)_3]Cl$ (**4**) (Scheme 2, path **a**). The clusters (**4a**−**e**) were obtained after chromatographic purification and recrystallization from chloroform/*n*-pentane as yellow, air-stable crystals in moderate yields (36−56%). In the reaction of **2a** with Me_2S_2, the formation of methyl chloride, *S*-methylthioacetate, and triphenylphosphine sulfide as side products were confirmed by GC/MS analyses as well as by NMR spectroscopy. These reactions proceeded with acetylplatinum(II) complexes

Scheme 1. General Method for the Synthesis of Acetylplatinum(II) Complexes **2** and Methylplatinum(II) Complexes **3** Starting from Platina-β-diketone **1**

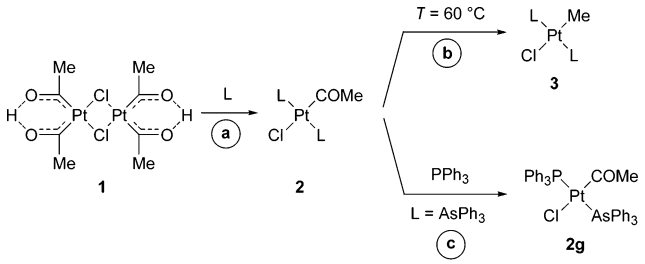

	2a	2b	2c	2d	2e	2f
L	PPh_3	$P(4\text{-}FC_6H_4)_3$	$AsPh_3$	$PMePh_2$	PMe_2Ph	PBu_3

	3a	3b	3c	3d
L	PPh_3	$P(4\text{-}FC_6H_4)_3$	$AsPh_3$	$PMePh_2$

containing the monodendate phosphine ligands PPh_3 (**2a**) and $P(4\text{-}FC_6H_4)_3$ (**2b**) in boiling chloroform within 2 days. The addition of Me_2S_2 to acetylplatinum(II) complexes containing the monodendate phosphine ligand $PMePh_2$ (**2d**) resulted in a decarbonylation reaction of the acetyl ligand giving the methyl(chloro)platinum(II) complex *trans*-$[Pt(Me)Cl(PMePh_2)_2]$ (**3d**), which was also observed in absence of Me_2S_2 (Scheme 1, path **b**). On the other hand, **2e** and **2f**, having PMe_2Ph and PBu_3 as ligands, did not react at all. This different reactivity may be due to the higher donor capability of $PMePh_2$, PMe_2Ph, and PBu_3 (Tolman's electronic parameter: $PMePh_2$, 2067.0 cm^{-1}; PMe_2Ph, 2065.3 cm^{-1}; PBu_3, 2060.3 cm^{-1}) compared to PPh_3 and $P(4\text{-}FC_6H_4)_3$ (Tolman's electronic parameter: PPh_3, 2068.9 cm^{-1}; $P(4\text{-}FC_6H_4)_3$, 2071.3 cm^{-1}).[16]

In contrast to this, the analogous reaction of **2a**−**2c** with diphenyldisulfide resulted in the formation of dinuclear platinum(II) complexes $[\{PtCl(L)\}_2(\mu\text{-}SPh)_2]$ (**5**) having the ligands PPh_3 (**5a**), $P(4\text{-}FC_6H_4)_3$ (**5b**), and $AsPh_3$ (**5c**) in mutual *trans* position (Scheme 2, path **b**). The reaction of **2a** with dibenzyldisulfide yielded after 48 h reaction time the cationic trinuclear platinum(II) complex $[\{Pt(PPh_3)\}_3(\mu_3\text{-}S)(\mu\text{-}SBn)_3]Cl$ (**6**) (Scheme 2, path **c**). It was proven by ESI−MS measurements that in the course of the reaction the trinuclear cluster $[\{Pt(PPh_3)\}_3(\mu\text{-}SBn)_3]Cl$ was also formed to a minor extend. The complexes **5a**−**c** and **6** were obtained after chromatographic purification and recrystallization from methylene chloride/*n*-pentane (**5a**), chloroform/*n*-pentane (**5b**, **5c**), and acetone/*n*-pentane (**6**) as yellow, air-stable crystals in moderate yields (16−44%).

The treatment of the acetylplatinum(II) complex **2c** (L = $AsPh_3$) with Me_2S_2 showed yet another reactivity yielding the dinuclear compound $[\{PtCl(AsPh_3)\}_2(\mu\text{-}SMe)_2]$ (**7**) (yield: 44%). The reaction of Me_2S_2 with the mixed triphenylphosphine-triphenylarsine complex **2g** (prepared as shown in Scheme 1, path **c**) gave four different triangular platinum clusters, $[\{Pt(PPh_3)\}_3(\mu\text{-}SMe)_3]Cl$ (**4a**), $[\{Pt(AsPh_3)\}\{Pt(PPh_3)\}_2(\mu\text{-}SMe)_3]Cl$ (**8a**), $[\{Pt(AsPh_3)\}_2\{Pt(PPh_3)\}(\mu\text{-}SMe)_3]Cl$ (**8b**), and $[\{Pt(AsPh_3)\}_3(\mu\text{-}SMe)_3]Cl$ (**8c**), in the ratio 43% (**4a**):39% (**8a**):15% (**8b**):3% (**8c**) (Scheme 3). The identities of clusters **4** as well as complexes **5**, **6**, and **7** were confirmed by microanalyses, ^1H, ^{13}C, ^{31}P NMR spectroscopy, and ESI−MS spectrometry. The clusters **8** were investigated by means of ^1H and ^{31}P NMR

(9) Jennings, M. C.; Schoettel, G.; Roy, S.; Puddephatt, R. J.; Douglas, G.; Manojlovic-Muir, L.; Muir, K. W. *Organometallics* **1991**, *10*, 580.
(10) Ramachandran, R.; Payne, N. C.; Puddephatt, R. J. *J. Chem. Soc. Chem. Commun*. **1989**, 128.
(11) Mingos, D. M. P.; Slee, T. *J. Organomet. Chem.* **1990**, *394*, 679.
(12) (a) Falvello, L. R.; Forniés, J.; Fortuno, C.; Durán, F.; Martin, A. *Organometallics* **2002**, *21*, 2226. (b) Bender, R.; Braunstein, P.; Dedieu, A.; Ellis, P. D.; Huggins, B.; Harvey, P. D.; Sappa, E.; Tiripicchio, A. *Inorg. Chem.* **1996**, *35*, 1223. (c) Leoni, P.; Marchetti, F.; Pasquali, M.; Marchetti, L.; Albinati, A. *Organometallics* **2002**, *21*, 2176.
(13) Imhof, D.; Venanzi, L. M. *Chem. Soc. Rev.* **1994**, 185.
(14) (a) Hadj-Bagheri, N.; Browning, J.; Dehghan, K.; Dixon, K. R.; Meanwell, N. J.; Vefghi, R. *J. Organomet. Chem.* **1990**, *396*, C47. (b) Mingos, D. M. P.; Williams, I. D.; Watson, M. J. *J. Chem. Soc. Dalton. Trans.* **1988**, 1509.
(15) Albrecht, C.; Wagner, C.; Merzweiler, K.; Lis, T.; Steinborn, D. *Appl. Organomet. Chem.* **2005**, *19*, 1155.
(16) Tolman C. A. *Chem. Rev.* **1977**, *77*, 313.

Scheme 2. Reactivity of Acetylplatinum(II) Complexes **2** toward Diorganodisulfides; Synthesis of Alkylthio Bridged 44 cve Triangular Platinum Clusters **4**, Dinuclear Arylthio Bridged Platinum(II) Complexes **5**, and the Trinuclear Benzylthio Bridged Platinum(II) Complex **6**

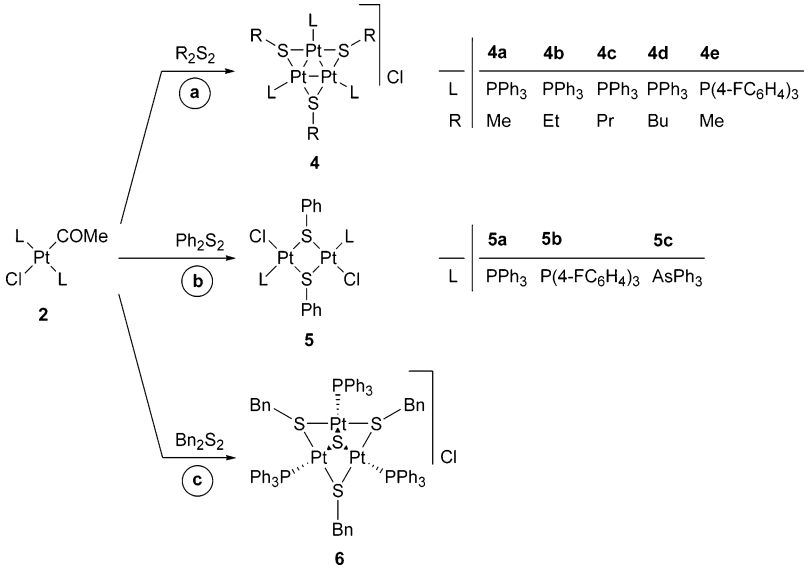

Scheme 3. Reactivity of Acetylplatinum(II) Complexes **2c** and **2g** toward Dimethyldisulfide

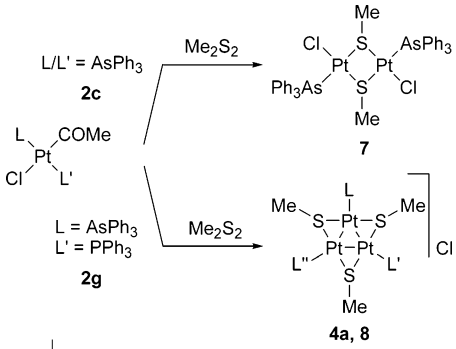

	4a	8a	8b	8c
L	PPh_3	$AsPh_3$	$AsPh_3$	$AsPh_3$
L'	PPh_3	PPh_3	$AsPh_3$	$AsPh_3$
L''	PPh_3	PPh_3	PPh_3	$AsPh_3$
ratio	43 %	39 %	15 %	3%

spectroscopy as well as by ESI−MS spectrometry. Furthermore, single-crystal X-ray diffraction analyses were performed for the compounds **4a**, **5c**, and **6**.

Structural Characterization. Suitable crystals for X-ray diffraction analysis of the triangular platinum cluster **4a** have been obtained from chloroform/*n*-pentane solutions as **4a**·$4CHCl_3$ (space group: $P2_1/n$). Crystals consist of discrete cations and anions without unusual intermolecular contacts. The structure of **4a**·$4CHCl_3$ is shown in Figure 1. Selected bond lengths and angles are given in the Figure caption.

The $Pt_3S_3P_3$-skeleton is essentially planar. The largest deviation from the Pt_3 plane amounts to 0.145(1) Å (S1). The arrangement of the platinum atoms approximate to an equilateral triangle (Pt−Pt−Pt 59.6(1)−60.3(1)°) with Pt−Pt distances between 2.887(1) and 2.907(1) Å. These distances are significantly longer than those in other higher symmetrical triangular platinum clusters (median 2.684 Å; lower/upper quartile 2.619/2.713 Å; $n = 18$).[17] The Pt−S bond lengths (Pt−S 2.288(1)−2.291(2) Å) are in the common range for platinum complexes with bridging *S*-alkyl groups (median 2.327 Å; lower/upper quartile 2.297/2.363 Å; $n = 16$). The Pt−S−Pt angles (78.2(1)−79.2(1)°) are remarkably small (other platinum complexes having bridging *S*-alkyl groups: Pt−S−Pt median 91.9°; lower/upper quartile 83.4/95.7°, $n = 24$), which indicates a higher ring strain in the Pt−S−Pt ring in **4a**. The methyl groups bonded to the sulfur atoms are arranged on the same side of the Pt_3-plane.

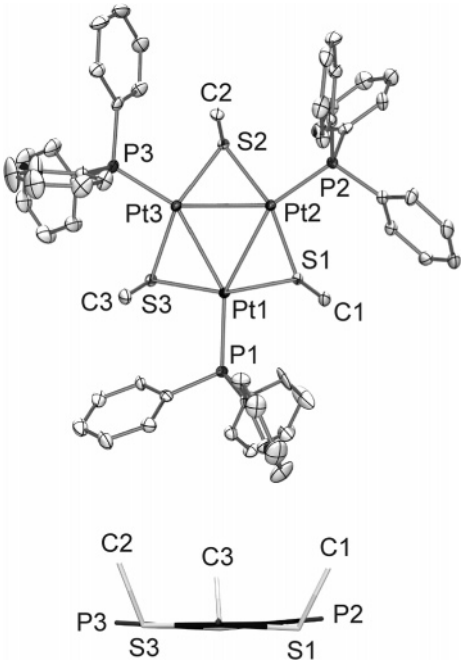

Figure 1. Molecular structure of $[\{Pt(PPh_3)\}_3(\mu\text{-}SMe)_3]^+$ in crystals of **4a**·$4CHCl_3$ with ellipsoids at the 30% probability level and stick model viewed along the Pt_3S_3 plane. H atoms are omitted for clarity. Selected distances (Å) and angles (deg): Pt1−Pt2 2.901(1), Pt1−Pt3 2.907(1), Pt2−Pt3 2.887(1), Pt1−P1 2.267(2), Pt2−P2 2.256(2), Pt3−P3 2.253(2), Pt1−S1 2.288(1), Pt1−S3 2.275(2), Pt2−S1 2.288(1), Pt2−S2 2.291(1), Pt3−S2 2.287(2), Pt3−S3 2.289(2), S1−C1 1.842(6), S2−C2 1.832(6), S3−C3 1.812(7), Pt1−Pt2−Pt3 60.3(1), Pt1−Pt3−Pt2 60.1(1), Pt2−Pt1−Pt3 59.6(1), Pt1−S1−Pt2 78.7(1), Pt1−S3−Pt3 79.1(1), Pt2−S2−Pt3 78.2(1).

(17) Cambridge Structural Database (CSD), University Chemical Laboratory, Cambridge.

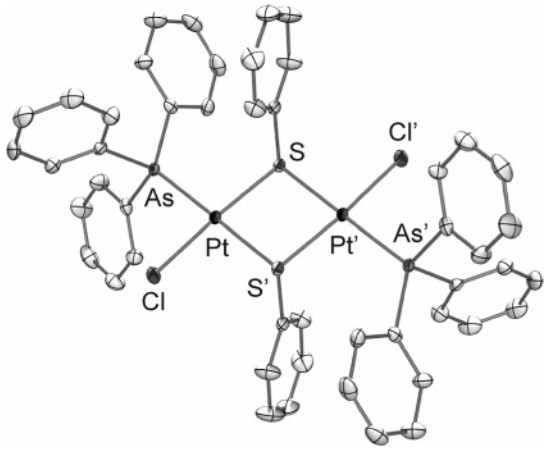

Figure 2. Molecular structure of $[\{PtCl(AsPh_3)\}_2(\mu\text{-}SPh)_2]$ in crystals of **5c**·$2CHCl_3$ with ellipsoids at the 30% probability level. H atoms are omitted for clarity. Selected distances (Å) and angles (deg): Pt−As 2.378(1), Pt−S 2.349(1), Pt−S′ 2.285(1), Cl−Pt 2.325(1), Cl−Pt−S 91.1(1), S−Pt−S′ 83.7(1), S−Pt−As 96.9(1), Cl−Pt−As 88.4(1), Pt−S−Pt 96.3(1).

The dinuclear complex **5c** crystallized from chloroform/diethyl ether as **5c**·$2CHCl_3$ in well-shaped yellow crystals that were suitable for single-crystal X-ray diffraction analysis (space group: $P2_1/n$). The crystal consists of discrete centrosymmetric molecules and is also without unusual intermolecular contacts. The structure of **5c**·$2CHCl_3$ is shown in Figure 2. Selected bond lengths and angles are given in the Figure caption.

The $Pt_2S_2As_2Cl_2$ core is approximately planar (largest deviation from the Pt_2S_2-plane: 0.029(1) Å for Cl). The Pt−S bond length trans to As (Pt−S 2.349(1) Å) reflects the lower trans influence of the $AsPh_3$ ligand compared to the PPh_3 ligand in **5a**·$2CHCl_3$ (Pt−S 2.370(2) Å).[16] The internal angles of the Pt_2S_2-ring (S−Pt−S′ 83.7(1)°, Pt−S−Pt′ 96.3(1)°) are comparable with those found in other dinuclear *S*-phenyl bridged platinum(II) complexes (S−Pt−S: median 82.7°; lower/upper quartile 81.3/82.9°; Pt−S−Pt: median 97.3°; lower/upper quartile 97.1/97.9°, $n = 8$).[18] The phenyl rings are situated nearly perpendicular to the planar Pt_2S_2 skeleton (angle between the Pt_2S_2 plane and the S−C1 vector 67.9(2)°) and were found to be in an anti position relative to the Pt_2S_2 frame.

The trinuclear complex **6** crystallized from acetone/*n*-pentane solutions as **6**·Me_2CO in well-shaped yellow crystals which were suitable for single-crystal X-ray diffraction analysis (space group: $P2_1/n$). The crystal consists of discrete molecules without unusual intermolecular contacts. The structure of **6**·Me_2CO is shown in Figure 3. Selected bond lengths and angles are given in the Figure caption.

The three platinum atoms span an equilateral triangle (Pt−Pt−Pt 59.6(1)−60.2(1)°) but the Pt···Pt distances in **6**·Me_2CO are significantly longer (3.044(1)−3.061(1) Å) than in the corresponding cluster **4a** by ca. 0.15 Å. This indicates a different type of Pt···Pt interaction in **6**·Me_2CO compared to clusters **4** as also confirmed by quantum chemical calculations (quod vide 2.4.). The planar Pt_3S_3 skeleton (largest deviation: 0.034(1) Å for Pt1) is capped by a sulfur atom (S4−CP 1.639(2) Å, Pt−S4−Pt 79.1(1)−79.5(1)°; CP = Pt_3S_3 plane). The Pt−S4 bond lengths are identical within the 3σ criterion (Pt−S4 2.390(2)−2.394(2) Å). Furthermore, the triphenylphosphine ligands are arranged below the Pt_3S_3 plane (P−CP 1.284(2)−1.457(2) Å, S4−Pt1−P1 176.7(1)°, S4−Pt2−P2 172.5(1)°), S4−Pt3−P3 177.1(1)°), whereas the benzyl groups are arranged above this plane (C1−CP 1.687(9) Å, C8−CP 1.692(9) Å, C15−CP 1.716(9) Å). The Pt−S bond lengths of the S−Bn groups (Pt−S 2.343(2)−2.356(2) Å) are longer and the Pt−S−Pt angles (Pt−S−Pt 80.8(1)−81.4(1)°) are larger than those in cluster **4a** (78.2(1)−79.2(1)°).

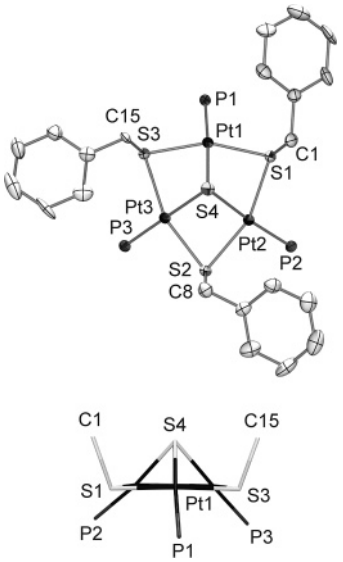

Figure 3. Molecular structure of $[\{Pt(PPh_3)\}_3(\mu_3\text{-}S)(\mu\text{-}SBn)_3]^+$ in crystals of **6**·Me_2CO with ellipsoids at the 30% probability level and stick model viewed along the Pt_3 plane. Phenyl rings of the phosphine ligands and H atoms are omitted for clarity. Selected distances (Å) and angles (deg): P1−Pt1 2.262(2), P2−Pt2 2.259(2), P3−Pt3 2.271(2), Pt1−S1 2.343(2), Pt1−S3 2.350(2), Pt1−S4 2.391(2), Pt2−S1 2.351(2), Pt2−S2 2.356(2), Pt2−S4 2.394(2), Pt3−S2 2.345(2), Pt3−S3 2.346(2), Pt3−S4 2.390(2), Pt3−Pt1−Pt2 60.2(1), Pt3−Pt2−Pt1 59.6(1), Pt1−Pt3−Pt2 60.2(1), Pt1−S1−Pt2 81.4(1), Pt3−S2−Pt2 81.2(1), Pt3−S3−Pt1 80.8(1), Pt3−S4−Pt1 79.1(1), Pt3−S4−Pt2 79.5(1), Pt1−S4−Pt2 79.5(1).

Spectroscopic Characterization. The ^{31}P NMR spectra and their simulation gave clear evidence of the constitution of the triangular platinum clusters $[(PtL)_3(\mu\text{-}SR)_3]Cl$ (L = PPh_3, R = Me−Bu, **4a**−**4d**; L = P(4-$FC_6H_4)_3$, R = Me, **4e**). Due to the natural abundance of the NMR active platinum isotope (^{195}Pt, 33.8%, $I = {}^1/_2$), the ^{31}P NMR spectra have to be analyzed as a superposition of the four spin systems A_3, A_2BX, ABB′XX′, and AA′A″XX′X″ (A, B = ^{31}P; X = ^{195}Pt) with central singlet resonances between −0.4 and 2.8 ppm (**4a**−**4e**). The measured ^{31}P NMR spectrum and the simulation of each spin system for the cluster **4a** are shown in Figure 4.

The trinuclear clusters **4** have several Pt−Pt, Pt−P, and P−P coupling pathways (e.g., for Pt−Pt: $^1J(Pt{-}Pt)$, $^2J(Pt{-}S{-}Pt)$, $^2J(Pt{-}Pt{-}Pt)$...; $^nJ(Pt,Pt) = \sum J(Pt,Pt)$). Due to the lack of knowledge concerning the signs as well as the exact determination of these magnitudes in the following, only the shortest coupling pathway is given. These coupling constants, illustrated in Table 1, were obtained by calculation using the PERCH program package.[19] Within the homologous series **4a**−**4d**, a dependency of the magnitude of the $^1J(Pt,Pt)$ coupling constant

(18) (a) Rivera, G.; Bernès, S.; Rodriguez de Barbarin, C.; Torrens, H. *Inorg. Chem.* **2001**, *40*, 5574. (b) Bruhn, C.; Becke, S.; Steinborn, D. *Acta Crystallogr. Sect. C* **1998**, *1102*. (c) Jain, V. K.; Kannan, S.; Butcher, R. J.; Jasinski, J. P. *J. Organomet. Chem.* **1994**, *468*, 285.

(19) (a) Annibale, G.; Bergamini, P.; Bertolasi, V.; Cattabriga, M.; Lazzaro, A.; Marchi, A.; Vertuani, G. *J. Chem. Soc. Dalton Trans.* **1999**, 3877. (b) Ma, E.; Semelhago, G.; Walker, A.; Farrar, D. H.; Gukathasan, R. R. *J. Chem. Soc. Dalton Trans.* **1985**, 2595.

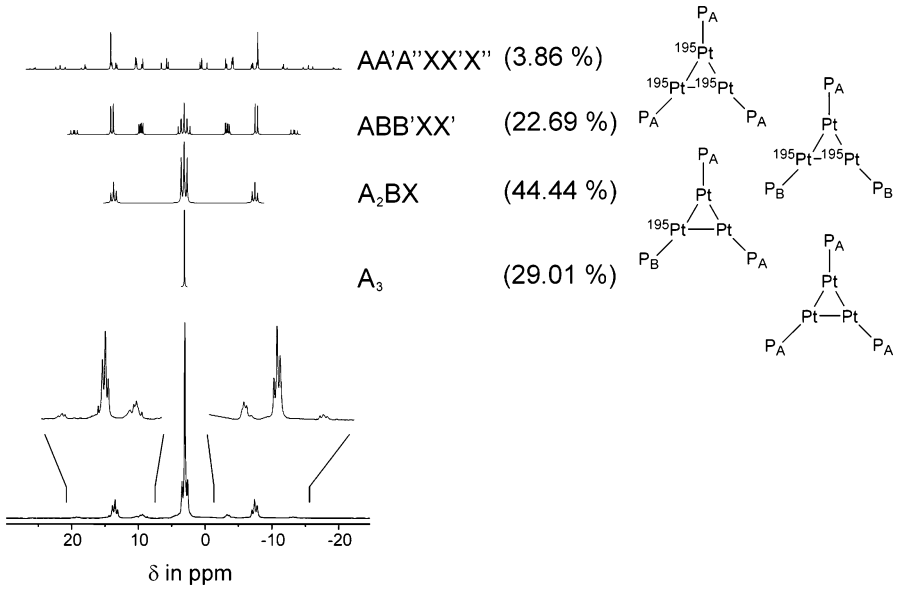

Figure 4. Observed and simulated ^{31}P NMR spectra of [{Pt(PPh$_3$)}$_3$(μ-SMe)$_3$]Cl (**4a**) along with the spin systems (A, B = ^{31}P; X = ^{195}Pt).

Table 1. Selected NMR Data (δ in ppm, J in Hz) for Triangular Platinum Clusters [(PtL)$_3$(μ-SR)$_3$]Cl (**4a**−**4e**, **9a**−**9d**)

L	R	δ(^{31}P)	^1J(^{195}Pt,^{31}P)	^1J(^{195}Pt,^{195}Pt)	^2J(^{195}Pt,^{31}P)	^3J(^{31}P,^{31}P)
PPh$_3$ (**4a**)	Me	2.8	4220	2100	96	80
PPh$_3$ (**4b**)	Et	1.4	4220	1950	96	81
PPh$_3$ (**4c**)	Pr	1.5	4240	1950	95	80
PPh$_3$ (**4d**)	Bu	1.4	4235	1930	97	80
P(4-FC$_6$H$_4$)$_3$ (**4e**)	Me	−0.4	4280	2250	100	80
PMePh$_2$ (**9a**)	Me	−16.4	4096	1900	85	75
PMe$_2$Ph (**9b**)	Me	−28.9	3956	*a*	*a*	*a*
PBu$_3$ (**9c**)	Me	−7.2	3930	1855	65	71
PBu$_3$ (**9d**)	Et	−8.1	3942	1810	67	71

a For intensity reasons, these coupling constants could not be obtained.

on the nature of the bridging sulfur ligand was found (^1J(Pt,-Pt): 2100 (**4a**, μ-SMe)−1930 Hz (**4d**, μ-SBu)). The signals for the SCH_3 protons of **4a** and **4e** should also be treated as the superposition of four spin systems. Temperature-dependent NMR measurements up to −50 °C gave no indication for an inversion of methyl groups at sulfur in complex **4a**.

The Pt−H coupling constants (^3J(Pt,H) = 43.6/42.7 Hz; **4a**/**4e**) are comparable with those found in *S*-methyl bridged dinuclear platinum complexes.[20,21] The carbon resonances of the methyl groups in **4a** and **4e** were found at 17.5 ppm (**4a**) and 18.4 ppm (**4e**) whereas the α-CH$_2$ groups in **4b**−**4d** resonate between 30.6 and 37.2 ppm.

To characterize the mixture of clusters [{Pt(AsPh$_3$)}{Pt-(PPh$_3$)}$_2$(μ-SMe)$_3$] (**8a**), [{Pt(AsPh$_3$)}$_2${Pt(PPh$_3$)}(μ-SMe)$_3$] (**8b**), and [{Pt(AsPh$_3$)}$_3$(μ-SMe)$_3$]Cl (**8c**) (Scheme 3), ESI−MS, ^{1}H, and ^{31}P NMR measurements were performed. The ESI−MS spectrum in the region of the isotopic patterns of the molecular cations indicated the presence of four clusters having mass differences of Δm = 44 amu (difference of the most intensive mass peaks [M]$^+$). This shows clearly the formation of **4a** (43%), **8a** (39%), **8b** (15%), and **8c** (3%), see Figure 5.

In the ^{31}P NMR spectrum, three multiplets (superposition of ^{31}P/^{195}Pt spin systems, analogous to that described above) with central singlet resonances at 3.0 ppm (**4a**), 3.6 ppm (**8a**), and 4.5 ppm (**8b**) were obtained. The ^{1}H NMR spectrum of clusters **8** showed two broad multiplets at 0.86 (superposition of **4a**, **8a**, **8b**) and 1.05 ppm (superposition of **8a**, **8b**, **8c**) in the area of the methyl protons.

The chemical equivalence of the phosphine ligands in **5a** and **5b** is evident from the ^{31}P NMR spectra showing multiplets with central singlet resonances at 19.3 ppm for **5a** and 15.8 ppm for **5b**. The Pt−Pt, Pt−P, and P−P coupling constants (^1J(Pt,P) = 3395/3303 Hz, ^2J(Pt,Pt) = 920/1230 Hz, ^3J(Pt,P) = −24/−39 Hz, ^4J(P,P) = 12/14 Hz; **5a**/**5b**) were obtained by calculation of the ABX and AA′XX′ (A, B = ^{31}P; ^{195}X = Pt) spin systems. The magnitudes of the ^2J(Pt,Pt) coupling constants were found to be positive, whereas the ^3J(Pt,P) coupling constants were found to be negative, as expected. In general, the sign of the ^2J(Pt,Pt) is mostly but not necessarily always positive whereas the sign of the ^3J(Pt,P) is negative.[22,23] The trans arrangement of the arsine ligands in **5c** and **7** follows from the ^{13}C NMR spectra especially from the isochronism of the carbon atoms of the two SPh groups in **5c** (δ_C = 128.5, *m*-*C*H; 130.5, *p*-*C*H; 131.0, *i*-*C*; 134.4, *o*-*C*H ppm) and of the two SCH_3 groups in **7** (δ_C = 19.0 ppm).

In the case of the sulfur capped trinuclear complex **6**, the identity was not only proven by a single-crystal X-ray diffraction measurement but also by NMR spectroscopic investigations. The ^{31}P NMR spectrum of **6** is treated as a superposition of four spin systems (A_3, A_2BX, ABB′XX′, AA′A″XX′X″; A, B = ^{31}P; ^{195}X = Pt) with a central singlet at 8.3 ppm. Coupling constants (^1J(Pt,P) = 3800 Hz, ^2J(Pt,Pt) = 458 Hz, ^3J(Pt,P) = −38 Hz, ^4J(P,P) = 6 Hz) were obtained by calculation. Remarkably, the magnitude of the Pt−Pt coupling constant (458 Hz) is much smaller than those in clusters **4** (1930−2250 Hz). This reflects clearly the different electronic nature as well as the bonding situation in compound **6** compared to clusters **4**. However, it has to be mentioned that the magnitudes of the

(20) PERCH-NMR-Software, 1993−2000 University of Kuopio, Version 1/2000.
(21) (a) Briant, C. E.; Gardner, C. J.; Hor, A. T. S.; Howells, T. S. N. G.; Mingos, D. M. P. *J. Chem. Soc. Dalton Trans.* **1984**, 2645. (b) Brown, M. P.; Puddephatt, R. J.; Upton, C. E. E. *J. Chem. Soc. Dalton Trans.* **1976**, 2490.
(22) (a) Kennedy, J. D.; McFarlane, W.; Puddephatt, R. J. *J. Chem. Soc. Dalton Trans.* **1976**, 745. (b) Kennedy, J. D.; Colquhoun, I. J.; McFarlane, W.; Puddephatt, R. J. *J. Organomet. Chem.* **1979**, *172*, 479.
(23) Pregosin, P. S. *Studies in Inorganic Chemistry 13, Transition Metal Nuclear Magnetic Resonance*; Elsevier: New York, 1991.

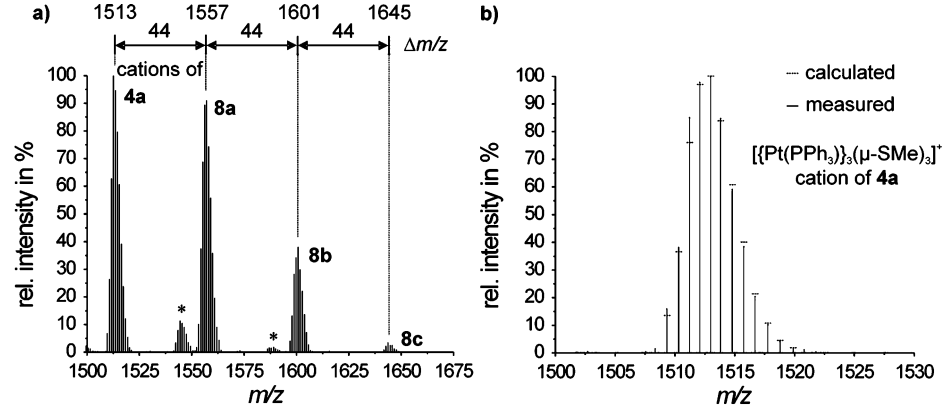

Figure 5. ESI−mass spectrum in MeOH from the reaction mixture of [Pt(COMe)Cl(AsPh$_3$)(PPh$_3$)] (**2g**) with Me_2S_2 in the area of $[M]^+$ (formation of [{Pt(AsPh$_3$)}{Pt(PPh$_3$)}$_2$(μ-SMe)$_3$] (**8a**), [{Pt(AsPh$_3$)}$_2${Pt(PPh$_3$)}(μ-SMe)$_3$] (**8b**), [{Pt(AsPh$_3$)}$_3$(μ-SMe)$_3$]Cl (**8c**), and [{Pt(PPh$_3$)}$_3$(μ-SMe)$_3$]Cl (**4a**)) as well as measured and calculated isotopic patterns of the cation of **4a** in the $[M]^+$ region (* = impurity).

Scheme 4. Substitution and Degradation Processes of Alkylthio Bridged 44 cve Triangular Platinum Clusters **4** in the Reactions with Phosphines

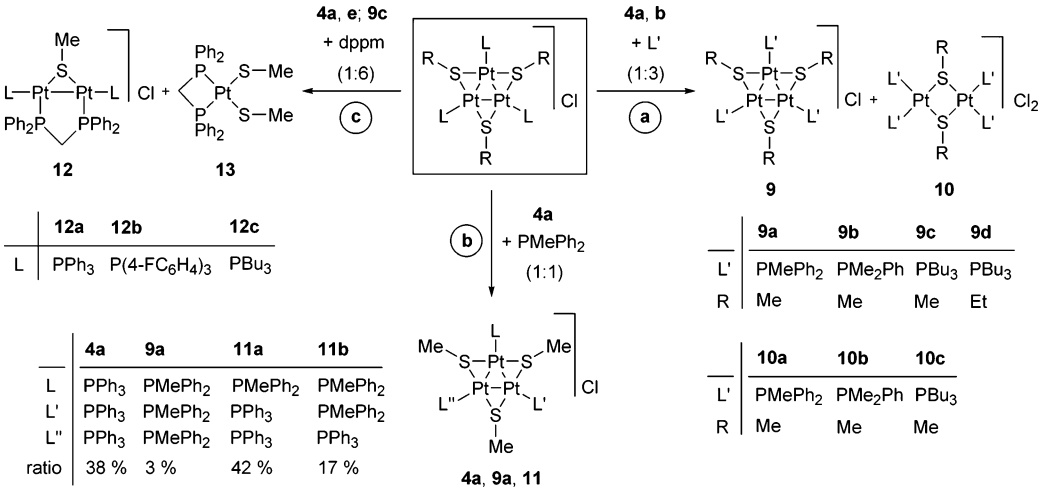

Pt−Pt coupling constants cannot be considered as an argument for a bond between the platinum atoms and in any event they do not correlate well with Pt−Pt distances.[23]

2.2. Reactivity of Triangular Platinum Clusters toward Phosphine Ligands. Triangular platinum clusters containing the monodentate phosphines $PMePh_2$, PMe_2Ph, and PBu_3 could not be prepared using the standard reaction procedure according to Scheme 2, path **a**. Therefore, we investigated whether clusters **4** are prone to ligand substitution. In fact, triangular platinum clusters [{Pt(PPh$_3$)}$_3$(μ-SR)$_3$]Cl (R = Me, **4a**; R = Et, **4b**) were found to react with three equivalents of $PMePh_2$, PMe_2Ph, and PBu_3 in chloroform at −70 °C, yielding a dark-red solution that changed color immediately to yellow upon warming to room temperature. ^{1}H and ^{31}P NMR measurements showed a complete substitution of the PPh_3 ligands yielding clusters [(PtL′)$_3$(μ-SR)$_3$]-Cl (R = Me, L′ = $PMePh_2$, **9a**; PMe_2Ph, **9b**; PBu_3, **9c**; R = Et, L = PBu_3, **9d**) (Scheme 4, path **a**).

These ligand substitution reactions are accompanied by partial degradation of the trinuclear clusters yielding dinuclear complexes [(PtL$_2$)$_2$(μ-SMe)$_2$]Cl$_2$ (L = $PMePh_2$, **10a**; PMe_2Ph, **10b**; PBu_3, **10c**). The formation of the fully substituted clusters **9a** and **9b** as well as the formation of dinuclear complexes **10a** and **10b** was proved by NMR spectroscopy, whereas clusters **9c** and **9d** were isolated as yellow oils after chromatographic purification, and the complex **10c** was obtained after reprecipitation from methylene chloride/*n*-pentane as a yellow powdery substance in moderate yields (48%, **9c**; 62% **9d**; 60%, **10c**). When the ligand substitution reaction is performed with a deficiency of $PMePh_2$ (**4a**: $PMePh_2$ = 1:1), some of the starting cluster **4a** remained in solution whereas both the partially substituted clusters **11a** and **11b** as well as the fully substituted cluster **9a** were formed (Scheme 4, path **b**). The constitutions of all clusters (**9**, **11**) as well as the dinuclear complexes **10** were revealed by NMR spectroscopy (^{1}H, ^{13}C, ^{31}P) and ESI−MS spectrometry.

In contrast to this, the addition of the bidentate phosphine ligand $PPh_2CH_2PPh_2$ (dppm) to a solution of clusters **4** and **9** in methylene chloride at −70 °C resulted in a fragmentation reaction yielding the cationic dinuclear platinum(I) complexes [(PtL)$_2$(μ-SMe)(μ-dppm)]Cl (**12**) (L = PPh_3, **12a**; P(4-FC$_6$H$_4$)$_3$, **12b**; PBu_3, **12c**), and the Pt(II) complex [Pt(SMe)$_2$(dppm)] (**13**) (Scheme 4, path **c**). These complexes were obtained after chromatographic purification as yellow crystals (**12a**, **12b**), yellow oil (**12c**), and light-yellow crystals (**13**), respectively. The identities of **12** and **13** were proven by ^{1}H, ^{13}C, and ^{31}P NMR spectroscopy as well as single-crystal X-ray diffraction analysis in the case of **12a**.

Structural and Spectroscopic Characterization. The ^{31}P NMR spectra of the fully substituted triangular platinum clusters [(PtL′)$_3$(μ-SR)$_3$]Cl (R = Me, L′ = $PMePh_2$, **9a**; PMe_2Ph, **9b**;

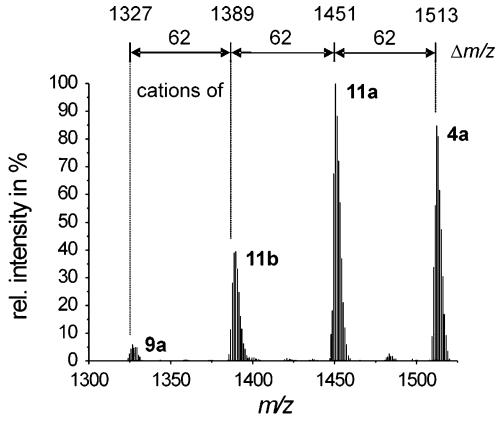

Figure 6. ESI−mass spectrum in CH_2Cl_2 from the reaction mixture of [{Pt(PPh$_3$)}(μ-SMe)$_3$]Cl (**4a**) and 1 equiv $PMePh_2$ in the $[M]^+$ region (measured 1 min after starting). The partially substituted clusters [{Pt(PMePh$_2$)}{Pt(PPh$_3$)}$_2$(μ-SMe)$_3$] (**11a**), [{Pt(PMePh$_2$)}$_2${Pt(PPh$_3$)}(μ-SMe)$_3$] (**11b**), and the fully substituted cluster [{Pt(PMePh$_2$)}$_3$(μ-SMe)$_3$]Cl (**9a**) were formed.

PBu_3, **9c**; R = Et, L = PBu_3, **9d**) are quite similar to those of clusters **4**. Central singlet resonances were found between −28.9 and −7.2 ppm (**9a**−**9e**). Magnitudes of Pt−Pt, Pt−P, and P−P coupling constants, which were obtained by calculation of the A_3, A_2BX, ABB′XX′, and AA′A″XX′X″ (A, B = ^{31}P; X = ^{195}Pt) spin systems, are also given in Table 1. To characterize the products in the reaction of **4a** with one equivalent $PMePh_2$, ^{31}P NMR spectroscopy and ESI−MS measurements were performed. In the ^{31}P NMR spectrum, two central singlet resonances at −16.8 (**9a**, **11**) and 3.0 (**4a**, **11**) ppm were obtained. The ESI−MS spectrum of the reaction mixture in the region of the isotopic patterns of the molecular cations is shown in Figure 6. This indicates clearly that during the course of the reaction three clusters in the ratio 38% (**11a**):17% (**11b**):3% (**9a**) were formed (Δm = 62 amu), whereas 42% of the starting material **4a** remained in solution.

The identities of the dinuclear complexes [(PtL$_2$)$_2$(μ-SMe)$_2$]Cl$_2$ (L = $PMePh_2$, **10a**; PMe_2Ph, **10b**; PBu_3, **10c**) follow from the chemical equivalence of the phosphine ligands in the ^{31}P NMR spectra (centered singlet resonances between −9.7 and 7.5 ppm) and from the resonances of the SCH_3 group in the ^{1}H NMR spectra.

Unambiguous proof of the constitution of the dinuclear platinum(I) complexes [(PtL)$_2$(μ-SMe)(μ-dppm)]Cl (**12**) (L = PPh_3, **12a**; P(4-FC_6H_4)$_3$, **12b**; PBu_3 **12c**) was acquired by NMR spectroscopy and X-ray diffraction measurements. Suitable crystals for X-ray diffraction analysis of **12a** have been obtained from chloroform/*n*-pentane solutions (space group: $P2_1/n$). The crystal structure of the cation of **12a** is shown in Figure 7. Selected bond lengths and angles are given in the Figure caption.

This crystal consists of discrete [{Pt(PPh$_3$)}$_2$(μ-SMe)(μ-dppm)]$^+$ cations and chloro anions without unusual intermolecular contacts. The Pt_2P_4S skeleton is in good approximation to a planar arrangement. The largest deviation from the Pt_2P_4S plane (CP) amounts to 0.099(2) Å (P2). The carbon atoms C1 and C2 are arranged on the same side of this plane (C1−CP 1.574(8) Å, C2−CP 0.721(9) Å). The Pt−Pt bond in **12a** (2.633(1) Å) is shorter than those in **4a** (2.887(1)−2.907(1) Å) but comparable with Pt−Pt distances in other dppm bridged platinum(I) complexes (Pt−Pt: median 2.648 Å, lower/upper

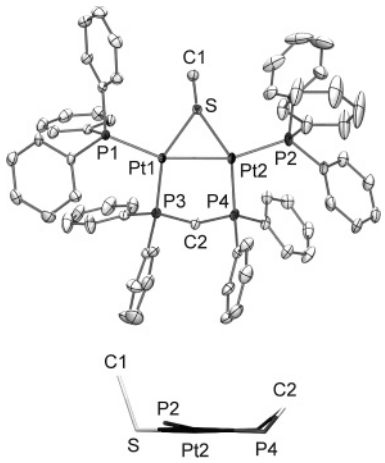

Figure 7. Molecular structure of [{Pt(PPh$_3$)}$_2$(μ-SMe)(μ-dppm)]$^+$ in crystals of **12a** with ellipsoids at the 30% probability level and stick model viewed along the Pt_2P_4S plane. H atoms are omitted for clarity. Selected distances (Å) and angles (deg): Pt1−Pt2 2.633(1), Pt1−P1 2.298(2), Pt1−P3 2.245(2), Pt2−P2 2.289(2), Pt2−P4 2.243(2), Pt1−S 2.297(2), Pt2−S 2.315(2), S−C1 1.802(8), P3−C2 1.821(8), P4−C2 1.840(8), P3−C2−P4 111.6(4), Pt1−S−Pt2 69.6(1).

quartile 2.580/2.707 Å).[24] The Pt−S−Pt-angle in **12a** is significantly smaller than those in **4a** (69.6(1)°, **12a**; 78.2(1)−79.2(1)°, **4a**). The P−C−P-angle of the dppm in **12a** (111.6(4)°) is enlarged by the bridging coordination mode compared to that of the uncoordinated dppm (106.2(1)°).[25]

Furthermore, NMR spectroscopic measurements provided clear evidence of the constitution of the dinuclear platinum(I) complexes **12**. The ^{31}P NMR spectra of **12** are treated as a superposition of the three spin systems AA′MM′, ABMNX, and AA′MM′XX′ (A, B, M, N = ^{31}P; X = ^{195}Pt). The ^{31}P NMR spectrum of the dinuclear platinum(I) complex **12c** as well as the simulation of these spin systems are shown in Figure 8.

Magnitudes of the Pt−Pt, Pt−P, and P−P coupling constants were obtained by calculation. Selected NMR data for all dinuclear platinum(I) complexes **12** are given in Table 2. Remarkably, all magnitudes of the ^2J(Pt,P*) and ^3J(P,P$^\#$) coupling constants (P* = dppm, P$^\#$ = L) are negative (^2J(Pt,P*) = −90 to −85 Hz; ^3J(P,P$^\#$) = −21 to −16 Hz), whereas the magnitudes of the *geminal-cis* ^2J(P*,P$^\#$) and the ^2J(P*,P*) coupling constants are positive (^2J(P*,P$^\#$) = 10−13 Hz; ^2J(P*,P*) = 25−40 Hz). The Pt−Pt coupling constants (^1J(Pt,Pt) = 2380−2850 Hz) are larger than those obtained in clusters **4** and **9** with R = Me (^1J(Pt,Pt) = 1810−2250 Hz). The assignment of the resonances is based on the fact that for all three complexes (**12a**−**12c**) the chemical shifts of the dppm signals (δ_P: −5.7 to −3.7 ppm) lie in a very narrow range whereas the resonances of the monodentate phosphine ligands were found between 3.5 and 21.9 ppm depending on the type of ligands. This is further confirmed by the magnitudes of the ^1J(Pt,P) coupling constants being between 3875 and 3925 Hz

(24) (a) Yip, H. K.; Che, C. M.; Peng, S. M. *J. Chem. Soc. Dalton Trans.* **1993**, 179. (b) Hong, X.; Yip, H. K.; Cheung, K. K.; Che, C. M. *J. Chem. Soc. Dalton Trans.* **1993**, 815. (c) Khan, M. N. I.; King, C.; Wang, J. C.; Wang, S.; Fackler, J. P., Jr. *Inorg. Chem.* **1989**, *28*, 4656. (d) Blau, R. J.; Espenson, J. H.; Kim, S.; Jacobson, R. A. *Inorg. Chem.* **1986**, *25*, 757. (e) Manojlovic-Muir, L.; Muir, K. W.; Solomun, T. *Acta Crystallogr. B* **1979**, *35*, 1237. (f) Manojlovic-Muir, L.; Muir, K. W.; Solomun, T. *J. Organomet. Chem.* **1979**, *179*, 479. (g) Brown, M. P.; Fisher, J. R.; Manojlovic-Muir, L.; Muir, K. W.; Puddephatt, R. J.; Thomson, M. A.; Seddon, K. R. *Chem. Commun.* **1979**, 931.
(25) Schmidbaur, H.; Reber, G.; Schier, A.; Wagner, F. E.; Müller, G. *Inorg. Chim. Acta* **1988**, *147*, 143.

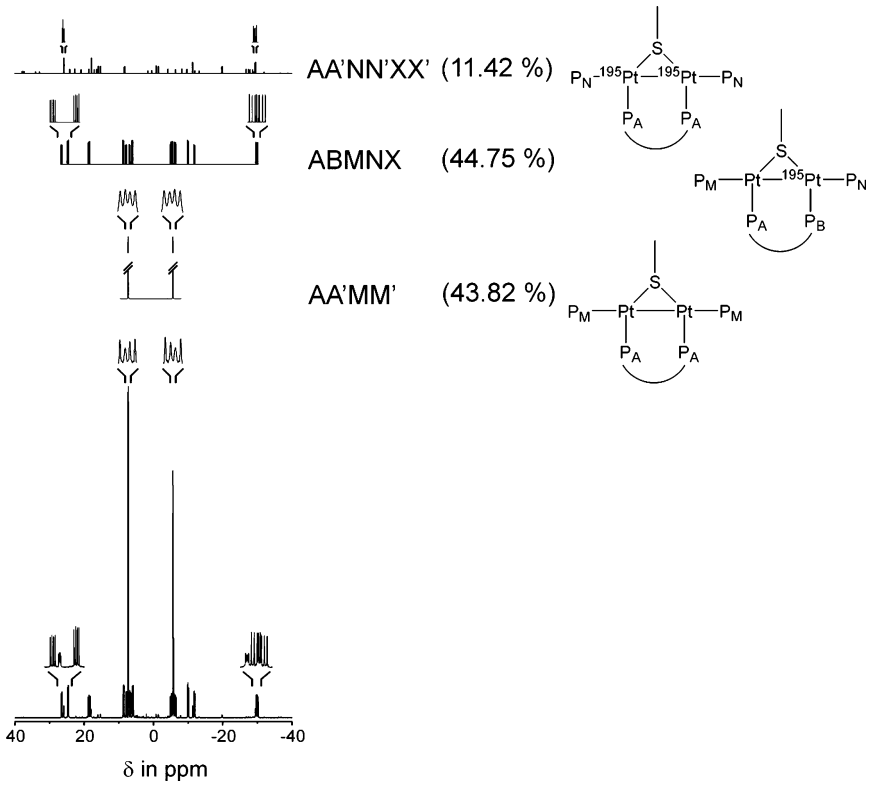

Figure 8. Observed and simulated ^{31}P NMR spectra of [{Pt(PBu$_3$)}$_2$(μ-SMe)(μ-dppm)]Cl (**12c**) along with the spin systems (A, B, M, N = ^{31}P; X = ^{195}Pt).

Table 2. Selected NMR Data (δ in ppm, J in Hz) for Dinuclear Platinum(I) Complexes [(PtL)$_2$(μ-SMe)(μ-dppm)]Cl (**12**) (P* = dppm, P$^{\#}$ = L)

L	δ(^{31}P) L	δ(^{31}P) dppm	^1J(Pt,Pt)	^1J(Pt,P$^{\#}$)	^1J(Pt,P*)	^2J(P*,P$^{\#}$)	^2J(P*,P*)	^3J(P$^{\#}$,P$^{\#}$)
PPh$_3$ (**12a**)	21.9	−3.9	2770	3010	3880	10	40	160
P(4-FC$_6$H$_4$)$_3$ (**12b**)	19.9	−3.7	2850	3055	3875	13	30	170
PBu$_3$ (**12c**)	7.3	−5.7	2380	2948	3925	10	25	150

for dppm (for comparison [{Pt(PPh$_3$)}$_2$(μ-SMe)(μ-dppm)]I: 3896 Hz) as well as between 2948 and 3055 Hz for the terminal *P*-ligands ([{Pt(PPh$_3$)}$_2$(μ-SMe)(μ-dppm)]I: 3040 Hz).[26]

The resonances of the SCH$_3$ groups of **12** (δ_H: 1.31−2.66 ppm, δ_C: 22.1−23.9 ppm) as well as the magnitudes of the ^3J(Pt,H) coupling constants (41.5−43.6 Hz) lie within the narrow range found for other *S*-methyl bridged dinuclear platinum complexes.[19,21]

In the ^{1}H NMR spectra of the complexes **12**, broad singlet resonances between 2.27 and 2.38 ppm were found in the area of the PPh$_2$C*H*$_2$PPh$_2$ groups. Due to the chemical inequivalence of these protons and the superposition of three highly complex spin systems (ABMM′OO′, ABMNOPX, ABMM′OO′XX′; A, B = ^{1}H, M, N, O, P = ^{31}P, X = ^{195}Pt), the coupling constants could not be obtained.

The identity of [Pt(SMe)$_2$(dppm)] (**13**) follows from the singlet resonances in the ^{31}P NMR spectrum at −47.0 ppm and from the triplet pattern of the SC*H*$_3$ protons (^4J(P,H) = 5.0 Hz) in the ^{1}H NMR spectrum, respectively. The resonance of the PPh$_2$C*H*$_2$PPh$_2$ group in **13** exhibited a triplet pattern at 4.28 ppm (^2J(P,H) = 10.4 Hz), which indicates the chemical equivalence of these protons in solution.

(26) Hunt, C. T.; Matson, G. B.; Balch, A. L. *Inorg. Chem.* **1981**, *20*, 2270.

Scheme 5. Reactivity of Alkylthio Bridged 44 cve Triangular Platinum Clusters **4** toward Halogens and Chalcogens

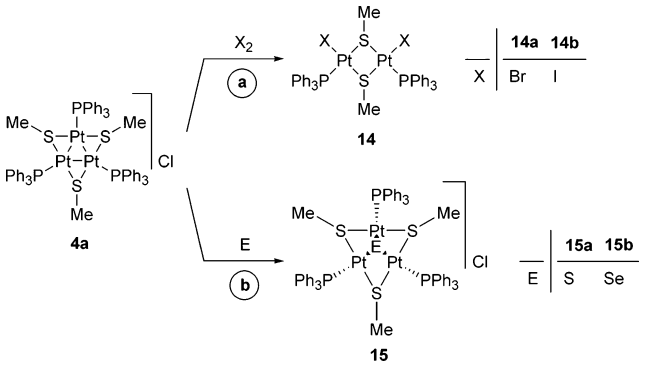

2.3. Oxidation Reactions of Triangular Platinum Clusters with Halogens and Chalcogens. To investigate the reactivity of the triangular platinum clusters **4** toward halogens and chalcogens the cluster **4a** was treated with bromine, iodine, sulfur, and selenium, respectively. The subsequent purification using preparative centrifugal thin layer chromatography revealed, in the case of halogens (X$_2$ = Br$_2$, I$_2$), the formation of the dinuclear platinum(II) complexes [{PtX(PPh$_3$)}$_2$(μ-SMe)$_2$] (**14**) (Scheme 5, path **a**) and, in the case of chalcogens (E = S, Se), the trinuclear platinum(II) complexes [{Pt(PPh$_3$)}$_3$(μ_3-E)(μ-SMe)$_3$]Cl (**15**) (Scheme 5, path **b**). The oxidation of **4a** with halogens proceeded in methylene chloride at −70 °C by slowly adding a solution of the requisite halogen in methylene chloride, whereas the oxidation with chalcogens required higher temperatures. These reactions were performed in benzene at 70 °C over a period of 2 days. The constitution of all complexes was unambiguously proved by NMR (^{1}H, ^{13}C, and ^{31}P) and IR spectroscopy, microanalyses, and for **15** also by ESI−MS

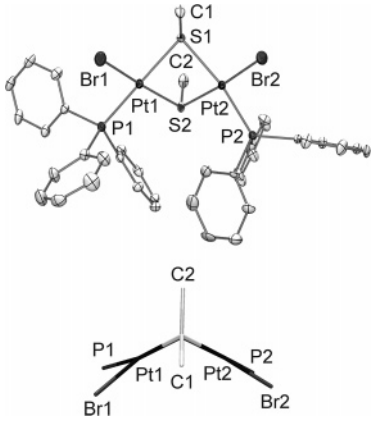

Figure 9. Molecular structure of $[\{PtBr(PPh_3)\}_2(\mu\text{-}SMe)_2]$ in crystals of **14a**·CH_2Cl_2 with ellipsoids at the 30% probability level and stick model viewed along the S1···S2 axis. H atoms are omitted for clarity. Selected distances (Å) and angles (deg): Pt1−P1 2.267(2), Pt2−P2 2.267(2), Pt1−Br1 2.460(1), Pt2−Br2 2.429(1), Pt1−S1 2.295(2), Pt1−S2 2.372(2), Pt2−S1 2.288(2), Pt2−S2 2.374(2), S1−C1 1.913(9), S2−C2 1.809(9), P1−Pt1−Br1 92.0(1), P2−Pt2−Br2 96.3(1), S1−Pt1−S2 79.1(1), S1−Pt2−S2 79.2(1), Pt1−S1−Pt2 90.2(1), Pt1−S2−Pt2 86.3(1).

spectrometry. Furthermore, for the compound **14b** a single-crystal X-ray diffraction analysis was performed.

Structural and Spectroscopic Characterization. Suitable crystals for X-ray diffraction analysis of **14a** have been obtained from methylene chloride/*n*-pentane solutions as **14a**·CH_2Cl_2 (space group: $P\bar{1}$). This crystal consists of discrete molecules without unusual intermolecular contacts. The structure of the dinuclear complex **14a**·CH_2Cl_2 revealed a hinged square-planar geometry (Figure 9). Selected bond lengths and angles are given in the Figure caption.

The coordination geometry about each platinum center is in good approximation with a square planar arrangement (sum of angles: Pt1 360.1°, Pt2 360.0°; angles between neighbored ligands: Pt1 79.1(1)−95.8(1), Pt2 79.2(1)−96.3(1)°). The Pt−Br bond lengths (Pt1−Br1 2.460(1), Pt2−Br2 2.429(1) Å) are as long as those in other platinum complexes having sulfur ligands in mutually trans positions (median 2.452 Å; lower/upper quartile 2.426/2.470 Å; $n = 62$). The Pt1−S1···S2−Pt2 dihedral angle (129.2(1)°) is a measure of the hinge distortion. In similar dinuclear complexes, the hinge distortions were found between 124 and 148°.[27] The bridging sulfur atoms in **14a**·CH_2Cl_2 are tetrahedral; the methyl groups have an anti type geometry.

Furthermore, the constitution and the geometry of complexes **14** is evident from the two resonances of the SCH_3 group in the ^{1}H NMR (d_H: 2.67, 2.77 ppm, **14a**; 2.75, 3.06 ppm, **14b**) as well as in the ^{13}C NMR spectra (δ_C: 14.4, 19.1 ppm, **14a**; 10.1, 19.0 ppm, **14b**). The chemical equivalence of the phosphine ligands is evident from the centered singlet resonances in the ^{31}P NMR spectrum (14.8/14.9 ppm **14a**/**14b**). Magnitudes of the Pt−P and P−P coupling constants (^1J(Pt,P) = 3298/3239 Hz, ^2J(Pt,Pt) = 820/960 Hz, ^3J(Pt,P) = −2 Hz/−2 Hz, ^4J(P,P) = 7/8 Hz; **14a**/**14b**) were obtained by calculation of the ABX and AA′XX′ (A, B = ^{31}P; X = ^{195}Pt) spin systems using the PERCH program package. Remarkably, the smaller values of the ^4J(P,P) in **14** compared to those found in **5** clearly show the cis arrangement of the phosphine ligands in **14**.

(27) (a) Chong, S. H.; Tjindrawan, A.; Hor, T. S. A. *J. Mol. Catal. A* **2003**, *204*, 267. (b) Mas-Balleste, R.; Capdevila, M.; Champkin, P. A.; Clegg, W.; Coxall, R. A.; Lledos, A.; Megret, C.; Gonzalez-Duarte, P. *Inorg. Chem.* **2002**, *41*, 3218. (c) Jones, W. D.; Reynolds, K. A.; Sperry, C. K.; Lachicotte, R. J.; Godleski, S. A.; Valente, R. R. *Organometallics* **2000**, *19*, 1661.

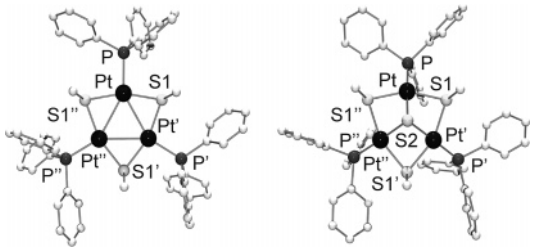

Figure 10. Calculated structures of the cations $[\{Pt(PPh_3)\}_3(\mu\text{-}SMe)_3]^+$ (**4a′**) and $[\{Pt(PPh_3)\}_3(\mu_3\text{-}S)(\mu\text{-}SMe)_3]^+$ (**15a′**). Selected distances (Å) and angles (deg) for **4a′**/**15a′**: Pt−Pt′ 2.933/3.134, Pt−S1 2.314/2.383, Pt−S1′ 2.325/2.387, Pt1−S2 −/2.402, Pt−P 2.276/2.281, S−C 1.830/1.826, Pt−Pt′−Pt″ 60.0/60.0, Pt−S1−Pt′ 78.4/82.1, Pt−S2−Pt′ −/81.4, S1−Pt−Pt′ 50.6/49.0, Pt″−Pt−S1″ 50.9/48.9, S1−Pt−S2 −/83.2, S2−Pt−S1″ −/83.1, S1″−Pt−P 100.0/96.0, P−Pt−S1 98.5/99.0.

Table 3. Selected NMR Data (δ in ppm, J in Hz) for Trinuclear Platinum Complexes $[\{Pt(PPh_3)\}_3(\mu_3\text{-}E)(\mu\text{-}SR)_3]Cl$ (**6**, **15a**, and **15b**)

E	R	$\delta(^{31}P)$	$^1J(^{195}Pt,^{31}P)$	$^2J(^{195}Pt,^{195}Pt)$	$^3J(^{195}Pt,^{31}P)$	$^3J(^{31}P,^{31}P)$
S (**6**)	Bn	8.3	3800	458	−40	6
S (**15a**)	Me	8.7	3808	480	−40	6
Se (**15b**)	Me	5.9	3937	400	−38	5

Selected NMR data of complexes **15** are shown in Table 3. The ^{31}P NMR spectra of **15** must be analyzed as a superposition of four spin systems (A_3, A_2BX, ABB′XX′, AA′A″XX′X″; A, B = ^{31}P; X = ^{195}Pt) with centered signals at 8.7 (**15a**) and 5.9 ppm (**15b**). The obtained coupling constants (^1J(Pt,P) = 3808/3937 Hz, ^2J(Pt,Pt) = 480/400 Hz, ^3J(Pt,P) = −40/−38 Hz, ^4J(P,P) = 6/5 Hz; **15a**/**15b**) are quite similar to those obtained for complex **6**.

2.4. Theoretical Calculations. The cations of complexes **4a** ($[\{Pt(PPh_3)\}_3(\mu\text{-}SMe)_3]^+$, **4a′**) and **15a** ($[\{Pt(PPh_3)\}_3(\mu_3\text{-}S)(\mu\text{-}SMe)_3]^+$, **15a′**) have been calculated on the DFT level of theory to understand the nature of bonding in the two different Pt_3 complexes. The calculated structures of **4a′** and **15a′** are shown in Figure 10. Selected bond lengths and angles are given in the Figure caption.

In the case of complex **4a**, structural data was available as a starting point and for comparison of the final structural parameters to judge the quality of calculations. The calculated and experimental structures were found to be in good agreement (largest deviation from Pt−Pt: 0.046 Å; Pt−S: 0.037 Å; Pt−P: 0.023 Å). In the case of compound **15a**, no crystal structure was available for direct comparison, but the similar trinuclear complex $[\{Pt(PPh_3)\}_3(\mu_3\text{-}S)(\mu\text{-}SBn)_3]^+$ (**6**) has been structurally characterized. Nevertheless, bond lengths and angles of the core of both structures are in good agreement.

The topological analysis of the electronic charge density $\rho(r)$ using the quantum theory of atoms in molecules (QTAIM) revealed a distinct difference regarding the Pt···Pt interaction in the two cations **4a′** and **15a′**. The trajetories of $\rho(r)$ of the molecules including bond paths, bond critical points (bcp's), and ring critical points (rcp's) are shown in Figure 11. In complex **4a′** (Figure 11, left) bcp's could be found between the metal centers. In addition, there were found rcp's in each of the Pt−Pt′−S rings and in the central Pt−Pt′−Pt″ ring. In sharp

Scheme 6. Survey Summary of the Synthesis and Reactivity of Alkyl-/Arylthio Bridged Di- and Trinuclear Platinum Complexes and Clusters

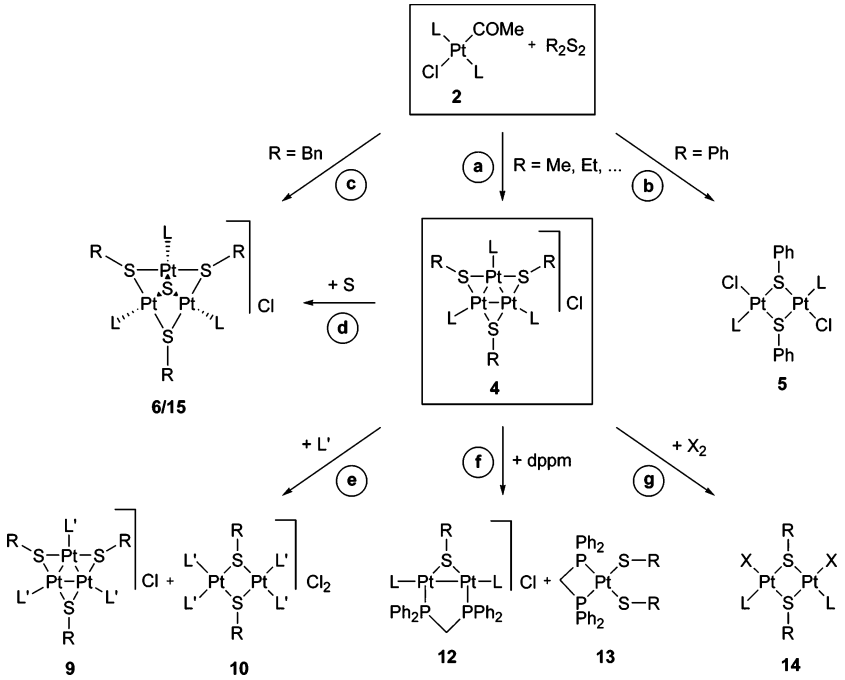

contrast, no bcp between the Pt atoms could be found in **15a′** (Figure 11, right).

The values found at the bond critical points show typical behavior for bonds incorporating heavy atoms.[28] The electron density is small, the Laplacian positive and small, $G/\rho < 1$, and $H/\rho < 0$. The high bond ellipticity ($\epsilon = 4.252$) at the Pt−Pt bcp's in **4a′** with the major axis parallel to the ring system suggests a strong delocalization of electron density in the plane of the ring system. The fact that the rcp's of the Pt−Pt′−S rings are in close vicinity to the Pt−Pt bond critical point indicates that the structure is close to a bifurcation catastrophe point (coalescence of bcp and rcp).[29]

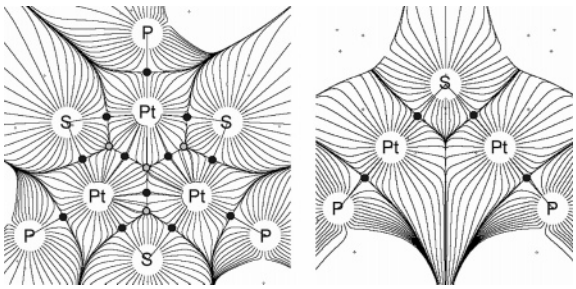

Figure 11. Gradient paths of electron density ρ(r) in the calculated structures of the cations **4a′** and **15a′** (● bond critical point {3, −1}, ○ (grey) ring critical point {3, 1}).

2.5 Discussion. In the scope of the work presented here, the synthesis of di- and trinuclear alkyl/arylthio bridged platinum complexes and clusters (Scheme 6, path **a**−**c**) and the reactivity of these clusters toward halogens, chalcogens, and phosphines (Scheme 6, path **d**−**g**) were explored. The triangular 44 cve platinum clusters **4** were obtained in reactions of **2** with dialkyldisulfides (Scheme 6, path **a**). Alkyl chloride, *S*-alkylthioacetate, dialkyl sulfide, and triphenylphosphine sulfide (in the case of **2a**) were identified as side products in all of these reactions. The platinum atoms in **4** exhibit the mean oxidation state +4/3; thus, they can be regarded formally in the oxidation state $1 \times Pt^{II} + 2 \times Pt^{I}$. In reactions of the acetyl complexes **2** with Ph_2S_2, the dinuclear arylthio bridged platinum(II) complexes **5** and *S*-phenylthioacetate as side products were received (Scheme 6, path **b**). Alternatively, Bn_2S_2 was found to react directly yielding the trinuclear sulfur capped platinum(II) complex **6** (Scheme 6, path **c**).

Although the mechanism of these reactions has not yet been investigated, a tentative path of formation can be given (Scheme 7).

Formation of Complexes 5 (Scheme 6, path b). The first step in the formation of **5** is probably the associative substitution of a phosphine ligand L by the disulfide R_2S_2 (**2** → **17**). In accordance with this, complexes **2** containing stronger donating phosphine ligands L like $PMePh_2$, PMe_2Ph, and PBu_3 do not react at all, most likely because the ligand substitution (**2** → **17**) is hampered. The second step, an oxidative S−S addition of the disulfide could take place resulting in a platinum(IV) intermediate (**17** → **18**) followed by a reductive C−S elimination of MeCOSR yielding the dinuclear complexes **5/7** (**18** → **5/7**). For all these reactions, examples with other platinum complexes were described.[30,31]

Formation of 44 cve Clusters 4 (Scheme 6, path a). There are indications that dinuclear complexes of type **5/7** may also

(28) Macchi, P.; Sironi, A. *Coord. Chem. Rev.* **2003**, *238*−*239*, 383.
(29) Bader, R. F. W. *Chem. Rev.* **1991**, *91*, 893.

(30) (a) Treichel, P. M.; Rosenhein, L. D. *Inorg. Chem.* **1984**, *23*, 4018. (b) Berg, J. M.; Spira, D. J.; Hodgson, K. O.; Bruce, A. E.; Miller, K. F.; Corbin, J. L.; Stiefel, E. I. *Inorg. Chem.* **1984**, *23*, 3412. (c) Treichel, P. M.; Rosenhein, L. D.; Schmidt, M. S. *Inorg. Chem.* **1983**, *22*, 3960. (d) Treichel, P. M.; Rosenhein, L. D. *J. Am. Chem. Soc.* **1981**, *103*, 691. (e) Stiefel, E. I.; Miller, K. F.; Bruce, A. E.; Corbin, J. L.; Berg, J. M.; Hodgson, K. O. *J. Am. Chem. Soc.* **1980**, *102*, 3624. (f) Sigel, H.; Scheller, K. H.; Rheinberger, V. M.; Fischer, B. E. *J. Chem. Soc. Dalton Trans.* **1980**, 1022.
(31) (a) McKarns, P. J.; Heeg, M. J.; Winter, C. H. *Inorg. Chem.* **1998**, *37*, 4743. (b) Lewkebandara, T. S.; McKarns, P. J.; Haggerty, B. S.; Yap, G. P. A.; Rheingold, A. L.; Winter, C. A. *Polyhedron* **1998**, *17*, 1. (c) Boorman, P. M.; Merrit, C. L.; Nandana, W. A. S.; Richardson, J. F. *J. Chem. Soc. Dalton Trans.* **1986**, 1251. (d) Roesky, H. W.; Gries, T.; Jones, P. G.; Weber, K.-L.; Sheldrick, G. M. *J. Chem. Soc. Dalton Trans.* **1984**, 1781. (e) Boorman, P. M.; Kerr, K. A.; Kydd, R. A.; Moynihan, K. J.; Valentine, K. A. *J. Chem. Soc. Dalton Trans.* **1982**, 1401.

Scheme 7. Proposed Mechanism for the Formation of Dinuclear Alkyl-/Arylthio Bridged Complexes **5/7**, Triangular Clusters **4**, and Trinuclear Complexes **6/15**

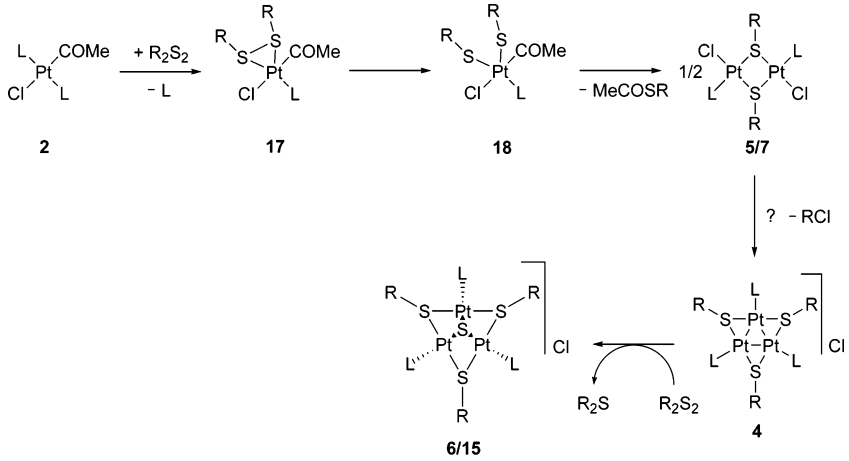

be intermediates in the formation of triangular clusters **4**: It was shown that in the reaction of the dinuclear alkylthio bridged complex **7** (R = Me, L = $AsPh_3$) with PPh_3 and Me_2S_2—among other complexes—the triangular cluster **4a** (R = Me, L = PPh_3) was also formed. Furthermore, MeCOSR is also yielded in the formation of complexes **4**. The side product RCl could be formed in a reduction step **5/7** ($2 \times Pt^{II}$) → **4** ($1 \times Pt^{II} + 2 \times Pt^{I}$).

Formation of the Trinuclear Complexes 6/15 (Scheme 6, path c, d). It is conceivable that the formation of complex [{Pt(PPh_3)}$_3$(μ_3-S)(μ-SBn)$_3$]Cl (**6**) in the reaction of **2a** with Bn_2S_2 (Scheme 6, path **c**) proceeds via oxidation of the corresponding cluster [{Pt(PPh_3)}$_3$(μ-SBn)$_3$]Cl (**4f**) by sulfur followed by the well-known disproportionation of the disulfide (Scheme 7, **4** → **6**/**15**).[32] In accordance with this, clusters **4** were found to be oxidized by sulfur and selenium yielding type **6**/**15** complexes (Scheme 6, path **d**). Furthermore, ESI−MS measurements showed that in the course of the reaction of **2a** with Bn_2S_2 the triangular platinum cluster **4f** and the sulfur capped trinuclear complex **6** were formed after 24 h in molar ratio 1:1.

To investigate the reactivity of these clusters, the parent cluster **4a** was treated with chalcogens (Scheme 6, path **d**), phosphine ligands (Scheme 6, path **e**, **f**), and halogens (Scheme 6, path **g**), resulting in oxidation, substitution, and degradation processes, respectively. Reactions of **4a** with monodentate phosphines L′ that are stronger donors than the leaving ligand L (L = PPh_3) gave rise to partial and/or full ligand substitution accompanied in all cases by a degradation yielding dinuclear complexes **10** (Scheme 6, path **e**). In the case of the bidentate phosphine ligand dppm, a degradation reaction took place yielding the dinuclear complex **12** and [Pt($SMe)_2$(dppm)] (**13**) (Scheme 6, path **f**). In this reaction, the mean oxidation state of Pt is preserved: **4** ($1 \times Pt^{II} + 2 \times Pt^{I}$) → **12** ($2 \times Pt^{I}$) + **13** ($1 \times Pt^{II}$). The observation of Chatt and Chini that the addition of phosphines L′ to the 42 cve clusters [{PtL}$_3$(μ-CO)$_3$] gives rise to the formation of red-colored 44 cve clusters [Pt_3L_3L'(μ-CO)$_3$][33] might indicate that the ligand substitution in our system (Scheme 6, path **e**, **f**) proceeds also via an addition elimination mechanism having 46 cve clusters [Pt_3L_3L'(μ-SMe)$_3$]Cl as intermediates.

Whereas **4a** was found to react with chalcogens in an oxidation reaction preserving the Pt_3S_3 core [**4a** ($1 \times Pt^{II} + 2 \times Pt^{I}$) → **15** ($3 \times Pt^{II}$)] (Scheme 6, path **d**), halogens were found to react with **4a** by oxidation coupled with degradation yielding the dinuclear platinum(II) complexes **14** (Scheme 6, path **g**). The structure of **14a** showed a hinge distortion of the central Pt_2S_2 ring (dihedral angle: 129.2(1)°). In contrast to the planar dinuclear Pt^{II} complexes **5**, complex **14a** might be stabilized by an intramolecular closed shell $Pt^{II}\cdots Pt^{II}$ ($d_{z^2}-d_{z^2}$) interactions (Pt···Pt 3.271(1) Å). Lledós and Alvarez showed by means of quantum chemical calculations with similar dinuclear platinum complexes that depending on the electronic and steric properties of the terminal ligands such closed shell interactions occur.[34]

To understand the nature of bonding in complexes of type **4** and **6**/**15**, quantum chemical calculations of the cations of the parent complexes **4a** and **15a** (L = PPh_3, R = Me) were performed. The existence of a bond path in the charge density—as found in **4a′** along the Pt−Pt vector—has been stated to be a necessary and sufficient requirement for the existence of a bond.[35] Thus, type **4** complexes have to be regarded as triangular 44 cve platinum clusters with Pt−Pt bonds whereas type **6**/**15** complexes are chalcogen-bridged trinuclear 48 ve complexes without Pt−Pt bonding interactions. Complexes **6**/**15** can be regarded as containing three square-planar platinum(II) moieties sharing one common monodentately bound ligand (μ_3-S). The sulfur atom in the trigonal-pyramidal Pt_3S unit is located 1.639(2) Å above the Pt_3 plane. With the planar five coordinated platinum centers in the non-oxidized clusters **4** in mind, the "capping" (**4** → **6**/**15**) results not only in the reduction of the coordination number (5 versus 4) but also in a severe change of the complex geometry. Thus, this oxidation reaction may be interpreted as a molecular switch of the complex geometry from planar to trigonal-pyramidal, whereas the coordination geometry of the platinum atoms remains planar in both cases.

(32) Démarcq, M. C. *J. Chem. Res.* **1993**, 3046.
(33) (a) Chatt, J.; Chini, P. *J. Chem. Soc. A* **1970**, 1538. (b) Albinati, A.; Carturan, G.; Musco, A. *Inorg. Chim. Acta* **1976**, *L2*. (c) Browning, C. S.; Farrar, D. H.; Gukathasan R. R.; Morris S. A. *Organometallics* **1985**, *4*, 1750.
(34) (a) González-Duarte, P.; Lledós, A.; Mas-Ballesté, R. *Eur. J. Inorg. Chem.* **2004**, 3585. (b) Mas-Ballesté, R.; Capdevila, M.; Champkin, P. A.; Glegg, W.; Coxall, R. A.; Lledós, A.; Mégret, C.; González-Duarte, P. *Inorg. Chem.* **2002**, *41*, 3218. (c) Aullón, G.; Ujaque, G.; Lledós, A.; Alvarez, S. *Chem.−Eur. J.* **1999**, *5*, 1391. (d) Aullón, G.; Ujaque, G.; Lledós, A.; Alvarez, S.; Alemany, P. *Inorg. Chem.* **1998**, *37*, 804. (e) Capdevila, M.; Clegg, W.; González-Duarte, P.; Jarid, A.; Lledós, A. *Inorg. Chem.* **1996**, *35*, 490.
(35) (a) Bader, R. F. W. *Atoms in Molecules: A Quantum Theory*; Clarendon Press: Oxford, U.K., 1990. (b) Bader, R. W. F. *Acc. Chem. Res.* **1985**, *18*, 9.

3. Experimental Section

3.1. General Comments. All reactions and manipulations were carried out under argon using standard Schlenk techniques. Solvents were dried prior to use: $CHCl_3$, CH_2Cl_2 over CaH_2, diethyl ether, pentane over Na benzophenone, and acetone over molecular sieve A4. The NMR spectra (^1H, ^{13}C, ^{19}F, ^{31}P, ^{195}Pt) were recorded at 27 °C on VARIAN Gemini 200, VXR 400, and Unity 500 spectrometers. Chemical shifts are relative to solvent signals ($CDCl_3$, δ_H 7.24, δ_C 77.0; CD_2Cl_2, δ_H 5.32, δ_C 53.8) as internal references; $\delta(^{31}P)$, $\delta(^{19}F)$, and $\delta(^{195}Pt)$ are relative to external H_3PO_4 (85% in D_2O), trifluorotoluene, and $H_2[PtCl_6]$ in D_2O, respectively. The coupling constants in higher order spin systems were calculated using the program PERCH 2000.[20] Microanalyses (C, H, S, Cl) were performed by the University of Halle microanalytical laboratory using for C, H, S a CHNS-932 (LECO) as well as a VARIO EL (Elementaranalysensysteme) elemental analyzers and for Cl by volumetric analysis (Schöninger). GC−MS analyses were carried out using a Hewlett-Packard (GC HP 5890 Series II, MS HP 5972) spectrometer equipped with mass selective detector (70 eV). IR spectra were recorded on a Galaxy FT−IR spectrometer Mattson 5000 using KBr pellets. ESI spectra were recorded on a Finnigan Mat spectrometer LCQ using the following conditions: carrier gas: N_2, flow rate: 8 μL/min, spray voltage: 4.1 kV, temperature of the capillary: 150 °C, voltage of the capillary: 34 kV. The preparative centrifugal thin layer chromatography was made by using a Chromatotron (Harrison Research). Hexachloroplatinic acid (Degussa) and phosphines (Aldrich, Fluka, Merck) were commercially available.

3.2. Reactivity of Platinum Acetyl Complexes toward Diorganodisulfides. 3.2.1. Preparation of Triangular Platinum Clusters [(PtL)$_3$(μ-SR)$_3$]Cl (4). To a solution of *trans*-[Pt(COMe)Cl(L)$_2$] (**2**) (0.50 mmol) in chloroform (7 mL) was added dialkyldisulfide (5.00 mmol). The reaction mixture was heated under reflux. After 48 h, the solvent and the excess of dialkyldisulfide were removed under vacuo. The residue was purified by preparative centrifugal thin layer chromatography using at first *n*-pentane/diethyl ether (5/1), then chloroform/diethyl ether (2/1), and finally chloroform/acetone (1/1) to elute the disulfide, phoshine sulfide, *S*-alkylthioacetate, alkyl chloride, and the complexes [(PtL)$_3$(μ-SR)$_3$]Cl (**4**), respectively. The latter complexes were dissolved in chloroform (3 mL) and reprecipitated with *n*-pentane (6 mL). After 2 days, the yellow, air-stable crystals were filtered off, washed with *n*-pentane (10 mL), and dried in vacuo.

[{Pt(PPh$_3$)}$_3$(μ-SMe)$_3$]Cl (4a). Yield: 150 mg (56%). Fp.: 123 °C, T_{dec}: 152 °C. Found: C, 42.30; H, 3.68; S, 6.19; Cl, 5.50. $C_{57}H_{54}S_3P_3ClPt_3 \cdot 0.5CHCl_3$ (1608.53) requires C, 42.93; H, 3.41; S, 5.98; Cl, 5.51. ^1H NMR (200 MHz, $CDCl_3$): δ 0.86 (m, ^3J(Pt,H) = 43.6 Hz, 9H, CH_3), 7.41 (s(br), 45H, *o*-, *m*-, *p*-C*H*). ^{13}C NMR (125 MHz, $CDCl_3$): δ 17.5 (s(br), *C*H$_3$), 128.6 (m, *m*-*C*H), 131.0 (m, *i*-*C*), 131.3 (s, *p*-*C*H), 133.9 (m, *o*-*C*H). ^{31}P NMR (202 MHz, $CDCl_3$): δ 2.8 (m, ^1J(Pt,P) = 4220 Hz, ^1J(Pt,Pt) = 2100 Hz, ^2J(Pt,P) = 96 Hz, ^3J(P,P) = 80 Hz). ^{195}Pt NMR (107 MHz, $CDCl_3$): δ −5767 (m). ESI−MS: *m*/*z* (obsd/calcd for [{Pt(PPh$_3$)}$_3$(μ-SMe)$_3$]$^+$, %) 1508 (1/1), 1509 (16/11), 1510 (38/36), 1511 (85/73), 1512 (98/97), 1513 (100/100), 1514 (85/83), 1515 (59/62), 1516 (39/40), 1517 (20/23), 1518 (10/11), 1519 (4/5) 1520 (2/2). IR: ν 3074(w), 3052(w), 2914(w), 1624(m), 1480(m), 1434(s), 1300(w), 1096(s), 746(m), 694(s), 534(s), 510(m) cm^{-1}. GC−MS of the reaction mixture: *m*/*z* (MeCl, %) 50 (100) (M$^+$), 47 (10), 40 (3), 37 (1), 35 (3). *m*/*z* (*S*-methylthioacetate, %) 90 (45) (M$^+$), 75 (5), 43 (100), 28 (13). *m*/*z* (Me_2S_2, %) 94 (100) (M$^+$), 79 (60), 64 (15), 61 (17), 45 (40), 33 (6), 28 (9).

[{Pt(PPh$_3$)}$_3$(μ-SEt)$_3$]Cl (4b). Yield: 135 mg (49%). T_{dec}: 143 °C. Found: C, 43.97; H, 4.00; S, 5.53. $C_{60}H_{60}S_3P_3ClPt_3 \cdot 0.5CHCl_3$ (1650.63) requires C, 44.03; H, 3.69; S, 5.83. ^1H NMR (200 MHz, $CDCl_3$): δ 0.42 (m(br), ^3J(H,H) = 7.15 Hz, 9H, CH_3), 1.19 (m, 6H, CH_2), 7.43 (m, 45H, Ph). ^{13}C NMR (125 MHz, $CDCl_3$): δ 21.1 (s+d, ^3J(Pt,C) = 44.5 Hz, *C*H$_3$), 30.6 (s(br), *C*H$_2$), 128.8 (m, *m*-*C*H), 131.3 (s, *p*-*C*H), 131.5 (m, *i*-*C*), 134.0 (m, *o*-*C*H). ^{31}P NMR (202 MHz, $CDCl_3$): δ 1.4 (m, ^1J(Pt,P) = 4220 Hz, ^1J(Pt,Pt) = 1950 Hz, ^2J(Pt,P) = 96 Hz, ^3J(P,P) = 81 Hz). IR: ν 3049(w), 2953(w), 2913(w), 2849(w), 1634(m), 1478(m), 1433(s), 1249(w), 1094(s), 747(m), 693(s), 532(s), 509(m) cm^{-1}.

[{Pt(PPh$_3$)}$_3$(μ-SPr)$_3$]Cl (4c). Yield: 113 mg (36%). T_{dec}: 142 °C. Found: C, 41.77; H, 3.96; S, 4.97. $C_{63}H_{66}S_3P_3ClPt_3 \cdot 2CHCl_3$ (1871.76) requires C, 41.71; H, 3.66; S, 5.14. ^1H NMR (500 MHz, $CDCl_3$): δ 0.22 (s(br), 9H, CH_3), 0.77 (s(br), 6H, β-CH_2), 1.13 (s(br), 6H, α-CH_2), 7.43 (m, 45H, Ph). ^{13}C NMR (125 MHz, $CDCl_3$): δ 13.0 (s, *C*H$_3$), 29.2 (s(br), β-*C*H$_2$), 37.2 (s(br), α-*C*H$_2$), 128.6 (s(br), *m*-*C*H), 131.3 (s(br), *p*-*C*H), 131.6 (m, *i*-*C*), 133.8 (s(br), *o*-*C*H). ^{31}P NMR (81 MHz, $CDCl_3$): δ 1.5 (m, ^1J(Pt,P) = 4240 Hz, ^1J(Pt,Pt) = 1950 Hz, ^2J(Pt,P) = 95 Hz, ^3J(P,P) = 80 Hz). ESI−MS: *m*/*z* (obsd/calcd for [{Pt(PPh$_3$)}$_3$(μ-SPr)$_3$]$^+$, %) 1592 (2/2), 1593 (10/11), 1594 (39/35), 1595 (73/71), 1596 (95/96), 1597 (100/100), 1598 (81/85), 1599 (62/64), 1600 (41/42), 1601 (24/25), 1602 (11/13), 1603 (5/6), 1604 (2/3). IR: ν 3048(w), 2957(w), 2915(w), 2867(w), 1478(m), 1433(s), 1227(w), 1094(s), 745(m), 692(s), 532(s), 510(m) cm^{-1}.

[{Pt(PPh$_3$)}$_3$(μ-SBu)$_3$]Cl (4d). Yield: 120 mg (42%). T_{dec}: 140 °C. Found: C, 45.61; H, 4.43; S, 5.73. $C_{66}H_{72}S_3P_3ClPt_3 \cdot 0.5\ CHCl_3$ (1717.05) requires C, 46.52; H, 4.26; S, 5.60. ^1H NMR (500 MHz, $CDCl_3$): δ 0.51 (s(br), 9H, CH_3), 0.59 (s(br), 6H, γ-CH_2), 0.88 (s(br), 6H, β-CH_2), 1.13 (s(br), 6H, α-CH_2), 7.44 (m, 45H, Ph). ^{13}C NMR (125 MHz, $CDCl_3$): δ 13.8 (s, *C*H$_3$), 21.9 (s, γ-*C*H$_2$), 29.6 (s, β-*C*H$_2$), 35.2 (s(br), α-*C*H$_2$), 128.5 (s(br), *m*-*C*H), 131.3 (s(br), *p*-*C*H, 131.4 (s(br), *i*-*C*), 133.7 (s(br), *o*-*C*H). ^{31}P NMR (81 MHz, $CDCl_3$): δ 1.4 (m, ^1J(Pt,P) = 4235 Hz, ^1J(Pt,Pt) = 1930 Hz, ^2J(Pt,P) = 97 Hz, ^3J(P,P) = 80 Hz). ESI−MS: *m*/*z* (obsd/calcd for [{Pt(PPh$_3$)}$_3$(μ-SBu)$_3$]$^+$, %) 1634 (2/2), 1635 (9/11), 1636 (39/34), 1637 (75/70), 1638 (98/95), 1639 (100/100), 1640 (88/85), 1641 (66/65), 1642 (43/43), 1643 (24/25), 1644 (11/13), 1645 (5/7), 1646 (2/3). IR: ν 3050(w), 2953(w), 2920(w), 2868(w), 1479(m), 1434(s), 1214(w), 1094(s), 745(m), 692(s), 532(s), 509(m) cm^{-1}.

[{Pt{P(4-FC$_6$H$_4$)$_3$}}$_3$(μ-SMe)$_3$]Cl (4e). Yield: 120 mg (42%). T_{dec}: 183 °C. Found: C, 39.64; H, 2.19. $C_{57}H_{45}S_3P_3F_9ClPt_3$ (1710.76) requires C, 40.02; H, 2.65. ^1H NMR (200 MHz, $CDCl_3$): δ 1.08 (m, ^3J(Pt,H) = 42.7 Hz, 9H, CH_3), 7.15 (m, 18H, Ph), 7.46 (m, 18H, Ph). ^{13}C NMR (125 MHz, $CDCl_3$): δ 18.4 (s(br), *C*H$_3$), 115.5 (d′t′, ^2J(C,F) = 20.2 Hz, N = 10.2 Hz, *m*-*C*H), 125.6 (′t′, N = 55.2 Hz, *i*-*C*), 137.0 (d′t′, ^3J(C,F) = 7.4 Hz, N = 16.6 Hz, *o*-*C*H), 165.5 (d, ^1J(C,F) = 254.1 Hz, *C*F). ^{31}P NMR (81 MHz, $CDCl_3$): δ −0.4 (m, ^1J(Pt,P) = 4280 Hz, ^1J(Pt,Pt) = 2250 Hz, ^2J(Pt,P) = 100 Hz, ^3J(P,P) = 80 Hz). ^{19}F NMR (188 MHz, $CDCl_3$): δ −106.9 (s(br)). IR: ν 3009(w), 2978(w), 2359(m), 2338(m), 1588(s), 1495(s), 1393(m), 1235(s), 1161(s), 1094(m), 827(m), 533(s) cm^{-1}.

3.2.2. Preparation of Dinuclear Platinum Complexes [{PtCl(L)}$_2$(μ-SPh)$_2$] (5). To a solution of (**2**) (0.50 mmol) in chloroform (7 mL) was added diphenyldisulfide (5.00 mmol). The reaction mixture was heated under reflux for 48 h. The solvent was then removed under vacuo. The residue was washed with *n*-pentane (5 × 10 mL) and purified by preparative centrifugal thin layer chromatography using at first *n*-pentane and finally diethyl ether/*n*-pentane (2/1) to elute Ph_2S_2, the phosphine ligand, and **5**, respectively. The last fraction was recrystallized from methylene chloride/*n*-pentane (1/10 mL) (**5a**) or chloroform/diethyl ether (1/10 mL) (**5b**, **5c**). After 2 days, the yellow, air-stable crystals were filtered off, washed with *n*-pentane (10 mL), and dried in vacuo.

[{PtCl(PPh$_3$)}$_2$(μ-SPh)$_2$] (5a). Yield: 47 mg (16%). T_{dec}: 196 °C. Found: C, 47.32; H, 3.35; S, 4.79; Cl, 5.13. $C_{48}H_{40}S_2P_2Cl_2Pt_2$ (1203.99) requires C, 47.88; H, 3.69; S, 4.79; Cl, 5.89. ^1H NMR (200 MHz, $CDCl_3$): δ 7.30 (m, Ph). ^{31}P NMR (81 MHz, $CDCl_3$): δ 19.3 (s+m, ^1J(Pt,P) = 3395 Hz, ^2J(Pt,Pt) = 920 Hz, ^3J(Pt,P) = −24 Hz, ^4J(P,P) = 12 Hz). ^{195}Pt NMR (107 MHz, $CDCl_3$): δ −4021 (m). IR: ν 3054(m), 1638(m), 1576(s), 1472(m), 1436(s), 1098(s), 1024(m), 738(m), 692(s), 536(s), 514(m) cm^{-1}.

[{PtCl{P(4-FC$_6$H$_4$)$_3$}}$_2$(μ-SPh)$_2$] (5b). Yield: 148 mg (45%). T_{dec}: 284−288 °C. ^1H NMR (200 MHz, $CDCl_3$): δ 6.93 (m, 18H, Ph), 7.40 (m, 12H, Ph), 7.64 (m, 4H, Ph). ^{13}C NMR (50 MHz,

$CDCl_3$): δ 115.5 (m, *m*-*C*H), 123.5 (m, SPh), 126.5 (s, SPh), 127.3 (m, *i*-*C*), 132.5 (s, SPh), 133.6 (m, SPh), 136.6 (m, *o*-*C*H), 164.2 (d,^1J(C,F) = 254.1 Hz, *C*F). ^{19}F NMR (188 MHz, $CDCl_3$): δ −108.1 (s). ^{31}P NMR (81 MHz, $CDCl_3$): δ 15.8 (s+m, ^1J(Pt,P) = 3303 Hz, ^2J(Pt,Pt) = 1230 Hz, ^3J(Pt,P) = −39 Hz, ^4J(P,P) = 14 Hz). IR: ν 3060(w), 2962(w), 1585(s), 1495(s), 1469(m), 1394(m), 1232(s), 1161-(s), 1095(s), 1016(m), 825(s), 744(m), 688(w), 528(s) cm^{-1}.

[{PtCl(AsPh$_3$)}$_2$(μ-SPh)$_2$] (5c). Yield: 47 mg (21%). T_{dec}: 252 °C. Found: C, 46.86; H, 3.72 $C_{48}H_{40}S_2As_2Cl_2Pt_2$·$Et_2O$ (1365.99) requires C, 46.26; H, 3.73. ^{1}H NMR (400 MHz, $CDCl_3$): δ 7.16 (m, 8H, Ph), 7.30 (m, 12H, Ph), 7.41 (m, 14H, Ph), 7.70 (m, 6H, Ph). ^{13}C NMR (100 MHz, $CDCl_3$): δ 128.5 (s, *m*-*C*H, SPh), 128.6 (s, *m*-*C*H, $AsPh_3$), 130.2 (s, *i*-*C*, $AsPh_3$), 130.3 (s, *p*-*C*H, $AsPh_3$), 130.5 (s, *p*-*C*H, SPh), 131.0 (s, *i*-*C*, SPh), 133.7 (s, *o*-*C*H, $AsPh_3$), 134.4 (s, *o*-*C*H, SPh). IR: ν 3051(w), 2919(w), 2850(w), 1481(m), 1436(s), 1079(m), 1023(w), 999(w), 738(s), 691(s) cm^{-1}.

3.2.3. Preparation of Trinuclear Complex [{Pt(PPh$_3$)}$_3$(μ_3-S)(μ-SBn)$_3$]Cl (6). To a solution of *trans*-[Pt(COMe)Cl(PPh_3)$_2$] (**2a**) (400 mg, 0.50 mmol) in chloroform (7 mL) was added dibenzyldisulfide (1.23 g, 5.00 mmol). The reaction mixture was heated under reflux. After 48 h, the solvent and the excess of dibenzyldisulfide were removed under vacuo. The residue was purified by preparative centrifugal thin layer chromatography using at first *n*-pentane/diethyl ether (5/1), then chloroform/diethyl ether (2/1), and finally chloroform/acetone/methanol (3/3/1) to elute Bn_2S_2, PPh_3S, and **6**, respectively. The latter complex was recrystallized from acetone/*n*-pentane solutions (3/6 mL). After 2 days, the light-yellow, air-stable crystals were filtered off, washed with *n*-pentane (10 mL), and dried in vacuo. Yield: 48 mg (16%). T_{dec}: 83 °C. Found: C, 48.52; H, 3.80. $C_{75}H_{66}S_4P_3ClPt_3$ (1809.20) requires C, 49.80; H, 3.68. ^{1}H NMR (500 MHz, $CDCl_3$): δ 1.24 (s(br), 6H, CH_2), 7.16 (m, 60H, Ph). ^{31}P NMR (81 MHz, $CDCl_3$): δ 8.3 (s+m, ^1J(Pt,P) = 3800 Hz, ^2J(Pt,Pt) = 458 Hz, ^3J(Pt,P) = −40 Hz, ^4J(P,P) = 6 Hz). ^{195}Pt NMR (107 MHz, $CDCl_3$): δ −3893 (m). ESI−MS: *m*/*z* (obsd/calcd for [{Pt(PPh$_3$)}$_3$(μ_3-S)(μ-SBn)$_3$]$^+$, %) 1768 (2/2), 1769 (12/10), 1770 (35/31), 1771 (70/65), 1772 (92/92), 1773 (100/100), 1774 (88/88), 1775 (68/70), 1776 (46/48), 1777 (28/30), 1778 (15/16), 1779 (10/8), 1780 (4/4). IR: ν 3052(w), 2924(w), 1479(m), 1434(s), 1096(s), 747(m), 694(s), 533(s), 512(m) cm^{-1}. ESI−MS of the reaction mixture after 24 h reaction time: *m*/*z* (obsd/calcd for [{Pt(PPh$_3$)}$_3$(μ-SBn)$_3$]$^+$, %) 1736 (2/2), 1737 (8/10), 1738 (32/32), 1739 (68/67), 1740 (92/93), 1741 (100/100), 1742 (86/87), 1743 (65/67), 1744 (47/45), 1745 (26/27), 1746 (13/14), 1747 (7/7), 1748 (3/3); (obsd/calcd for [{Pt(PPh$_3$)}$_3$(μ_3-S)(μ-SBn)$_3$]$^+$, %) 1768 (2/2), 1769 (12/10), 1770 (35/31), 1771 (70/65), 1772 (92/92), 1773 (100/100), 1774 (88/88), 1775 (68/70), 1776 (46/48), 1777 (28/30), 1778 (15/16), 1779 (10/8), 1780 (4/4). Relative ratio after 24 h reaction time calculated from ESI−MS spectrum: [{Pt(PPh$_3$)}$_3$(μ-SBn)$_3$]Cl : [{Pt(PPh$_3$)}$_3$(μ_3-S)(μ-SBn)$_3$]Cl, 1:1.

3.2.4. Preparation of Dinuclear Platinum Complex [{PtCl(AsPh$_3$)}$_2$(μ-SMe)$_2$] (7). To a solution of *trans*-[Pt(COMe)Cl($AsPh_3$)$_2$] (**2c**) (220 mg, 0.25 mmol) in chloroform (7 mL) was added dimethyldisulfide (236 mg, 2.50 mmol). The reaction mixture was heated under reflux for 48 h. The solvent was then removed under vacuo. The residue was purified by preparative centrifugal thin layer chromatography using at first *n*-pentane, then chloroform/acetone (1/1), and finally chloroform/acetone/methanol (1/1/1) to elute Ph_2S_2, $AsPh_3$, and **7**, respectively. From the last fraction, the solvent was removed in vacuo. The light-yellow powder was recrystallized from chloroform/*n*-pentane (10/10 mL) solutions. After 2 days, the light-yellow, air-stable crystals were filtered off, washed with *n*-pentane (10 mL), and dried in vacuo. Yield: 65 mg (44%). T_{dec}: 102 °C. Found: C, 39.07; H, 3.39; S, 5.39. $C_{38}H_{36}S_2As_2Cl_2Pt_2$ (1167.73) requires C, 39.09; H, 3.11; S, 5.49. ^{1}H NMR (400 MHz, $CDCl_3$): δ 2.51 (s+d, ^3J(Pt,H) = 39.0 Hz, 6H, CH_3), 7.29 (m, 12H, Ph), 7.39 (m, 6H, Ph), 7.52 (m, 12H, Ph). ^{13}C NMR (100 MHz, $CDCl_3$): δ 19.0 (s(br), *C*H$_3$), 128.7 (s, *m*-*C*H), 130.4 (s, *p*-*C*H), 131.0 (s, *i*-*C*), 133.7 (s, *o*-*C*H). IR: ν 3051(w), 2916(w), 2360-(m), 2339(m), 1481(m), 1435(s), 1079(m), 1024(w), 998(w), 956(w), 738(s), 692(s) cm^{-1}.

3.2.5. Reactivity of [Pt(COMe)Cl(AsPh$_3$)(PPh$_3$)] toward Me$_2$S$_2$. To a solution of *trans*-[Pt(COMe)Cl($AsPh_3$)(PPh_3)] (**2g**) (200 mg, 0.24 mmol) in chloroform (7 mL) was added dimethyldisulfide (236 mg, 2.50 mmol). The reaction mixture was heated under reflux for 48 h. The solvent was then removed under vacuo. The residue was purified by preparative centrifugal thin layer chromatography using at first *n*-pentane, then chloroform/acetone (1/1), and finally chloroform/acetone/methanol (1/1/1) to elute the disulfide, phoshine sulfide, *S*-alkylthioacetate, alkyl chloride, and the complexes [(PtL)$_3$(μ-SMe)$_3$]-Cl (**4a**, **8**), respectively. The trinuclear clusters **4a**, **8** were reprecipitated from chloroform/*n*-pentane solutions (2/15 mL). After 1 h, the yellow, air-stable powder was filtered off, washed with *n*-pentane (10 mL), and dried in vacuo. Yield: 74 mg. ^{1}H NMR (200 MHz, $CDCl_3$): δ 0.86 (m, 3.9 H (43%), CH_3 (**4a**, **8**)), δ 1.05 (m, 3.5H (39%), CH_3 (**8**)), 7.43 (s(br), 45H, Ph). ^{31}P NMR (81 MHz, $CDCl_3$): δ 3.0 (m, **4a**), 3.6 (m, **8a**), 4.5 (m, **8b**). ESI−MS: *m*/*z* (obsd/calcd for [$Pt_3(PPh_3)_2(AsPh_3)$-(μ-SMe)$_3$]$^+$ (cation of **8a**), %) 1552 (2/2), 1553 (11/12), 1554 (41/37), 1555 (75/73), 1556 (98/97), 1557 (100/100), 1558 (82/83), 1559 (61/62), 1560 (39/40), 1561 (22/24), 1562 (10/12), 1563 (5/6), 1564 (1/2); (obsd/calcd for [$Pt_3(PPh_3)(AsPh_3)_2$(μ-SMe)$_3$]$^+$ (cation of **8b**), %) 1597 (11/12), 1598 (35/37), 1599 (74/73), 1600 (90/97), 1601 (100/100), 1602 (79/83), 1603 (58/62), 1604 (36/40), 1605 (19/24), 1606 (7/6), 1607 (2/2); (obsd/calcd for [{Pt($AsPh_3$)}$_3$(μ-SMe)$_3$]$^+$ (cation of **8c**), %) 1639 (1/1), 1640 (2/2), 1641 (9/11), 1642 (35/37), 1643 (78/73), 1644 (100/97), 1645 (97/100), 1646 (83/83), 1647 (55/62), 1648 (41/42), 1649 (10/12), 1650 (6/6). Ratio calculated from ESI−MS spectrum: **4a**, 43%; **8a**, 39%; **8b**, 15%; **8c**, 3%.

3.3. Reactivity of Triangular Platinum Clusters [{Pt(PPh$_3$)}$_3$(μ-SR)$_3$]Cl (4). 3.3.1. Reactivity toward Monodendate Phosphine Ligands. Reaction of 4a with PMePh$_2$. To a solution of **4a** (100 mg, 0.065 mmol) in deuterated chloroform (0.7 mL) was added $PMePh_2$ (39 mg, 0.195 mmol) at −70 °C. Directly after the addition of the phosphine, a dark-red solution was formed. After warming up to room temperature, the color of the reaction mixture changed to yellow. This solution was investigated by NMR spectroscopy. ^{1}H NMR (200 MHz, $CDCl_3$): δ 1.33 (m, ^3J(Pt,H) = 44.8 Hz, CH_3S (**9a**)), 1.74 (s(br)+d, ^3J(Pt,H) = 36.5 Hz, SCH_3 (**10a**), 2.04 (m(br), CH_3P (**10a**)), 2.65 (m(br), CH_3P (**9a**)), 7.33 (m(br), Ph), 7.52 (m(br), Ph). ^{31}P NMR (81 MHz, $CDCl_3$): δ −16.4 (m,^1J(Pt,P) = 4096 Hz,^1J(Pt,Pt) = 1900 Hz, ^2J(Pt,P) = 85 Hz, ^3J(P,P) = 75 Hz, **9a**), −4.3 (s, PPh_3), 4.5 (s+m, ^1J(Pt,P) = 3012 Hz, ^3J(Pt,P) = −11 Hz, ^4J(P,P) = 15 Hz, **10a**). ESI−MS: *m*/*z* (obsd/calcd for [{Pt($PMePh_2$)}$_3$(μ-SMe)$_3$]$^+$ (cation of **9a**), %) 1323 (7/14), 1324 (37/40), 1325 (75/78), 1326 (92/100), 1327 (100/99), 1328 (80/80), 1329 (84/59), 1330 (83/36), 1331 (37/21), 1332 (26/10), 1333 (6/5).

Reaction of 4a with PMePh$_2$ in a Stoichiometric Ratio of 1:1 (Using 0.065 mmol of 4a and PMePh$_2$). ^{1}H NMR (200 MHz, $CDCl_3$): δ 0.86 (m(br), CH_3 (**4a**, **11**)), 1.33 (m(br), CH_3S (**9a**, **11**)), 2.65 (m(br), CH_3P (**9a**,**11**)), 7.33 (m(br), Ph), 7.30 (s(br), Ph), 7.52 (m(br), Ph). ^{31}P NMR (81 MHz, $CDCl_3$): δ −16.8 (m(br), **9a**, **11**), −4.3 (s, PPh_3), 3.0 (m(br), **4a**, **11**), 4.5 (s, **10a**). ESI−MS: *m*/*z* (obsd/calcd for [$Pt_3(PPh_3)_2(PMePh_2)$(μ-SMe)$_3$]$^+$ (cation of **11a**), %) 1446 (1/2), 1447 (10/12), 1448 (34/38), 1449 (68/75), 1450 (90/98), 1451 (100/100), 1452 (80/82), 1453 (57/61), 1454 (37/39), 1455 (21/23), 1456 (12/11), 1457 (6/6), 1458 (2/2); (obsd/calcd for [$Pt_3(PPh_3)(PMePh_2)_2$-(μ-SMe)$_3$]$^+$ (cation of **11b**), %) 1384 (1/2), 1385 (6/13), 1386 (29/39), 1387 (71/77), 1388 (99/99), 1389 (100/100), 1390 (84/81), 1391 (63/60), 1392 (41/38), 1393 (27/22), 1394 (13/11), 1395 (7/5), 1396 (3/2).

Reaction of 4a with PMe$_2$Ph. To a solution of **4a** (100 mg, 0.065 mmol) in deuterated chloroform (0.7 mL) was added PMe_2Ph (27 mg, 0.20 mmol) at −70 °C. Directly after the addition of the phosphine, a dark-red solution was formed, which changed color within 10 min to yellow. After warming up to room temperature, the solution was investigated by NMR spectroscopy. ^{1}H NMR (200 MHz, $CDCl_3$): δ

1.77 (′t′+d′t′, N = 5.0 Hz, ^3J(Pt,H) = 31.5 Hz, CH_3P; diastereotopic protons have not been found to split up to −50 °C), 2.41 (quin+dquin, ^3J(Pt,H) = 37.4 Hz, ^4J(P,H) = 2.5 Hz, CH_3S), 7.40 (m(br), Ph). ^{31}P NMR (81 MHz, $CDCl_3$): δ −28.9 (m, ^1J(Pt,P) = 3956 Hz, **9b**), −9.7 (s+m, ^1J(Pt,P) = 2996 Hz, ^3J(Pt,P) = −7 Hz, ^4J(P,P) = 14 Hz, **10b**), −4.3 (s, PPh_3). From this solution, the solvent was removed under vacuo, and the residue was purified by reprecipitation from methylene chloride/*n*-pentane solutions (2/7 mL). After 5 h, the light-yellow, air-stable powder of [{Pt(PMe_2Ph)$_2$}$_2$(μ-SMe)$_2$]Cl_2 (**10b**) was filtered off, washed with *n*-pentane (10 mL), and dried in vacuo. Yield: 65 mg (60%). ^{1}H NMR (200 MHz, $CDCl_3$): δ 1.77 (′t′+d′t′, N = 4.98 Hz, ^3J(Pt,H) = 31.5 Hz, 24H, CH_3P), 2.41 (quin+dquin, ^3J(Pt,H) = 37.4 Hz, ^4J(P,H) = 2.5 Hz, 6H, CH_3S), 7.40 (m(br), 30H, Ph). ^{31}P NMR (81 MHz, $CDCl_3$): −9.74 (s+m, ^1J(Pt,P) = 2996 Hz, ^3J(Pt,P) = −7 Hz, ^4J(P,P) = 14 Hz).

Reaction of 4a with PBu_3. To a solution of **4a** (100 mg, 0.065 mmol) in deuterated chloroform (0.7 mL) was added PBu_3 (39 mg, 0.20 mmol) at −70 °C. Directly after the addition of the phosphine, a dark-red solution was formed. After warming up to room temperature, the color of the reaction mixture changed to light yellow. This solution was investigated by NMR spectroscopy. ^{1}H NMR (200 MHz, $CDCl_3$): δ 0.79−0.89 (m, CH_3, **9c**, **10c**), 1.26−1.48 (m, CH_2, **9c**, **10c**), 1.69 (s(br), CH_2, **9c**), 1.86−2.07 (m, CH_2, CH_3, **9c**, **10c**), 2.36 (s+m, ^3J(Pt,H) = 47.3 Hz, SCH_3 (**9c**)), 7.30 (s(br), Ph). ^{31}P NMR (81 MHz, $CDCl_3$): δ −7.2 (m, ^1J(Pt,P) = 3930 Hz, ^1J(Pt,Pt) = 1855 Hz, ^2J(Pt,P) = 65 Hz, ^3J(P,P) = 71 Hz, **9c**), −4.3 (s, PPh_3), 7.5 (s+m, ^1J(Pt,P) = 2565 Hz, ^3J(Pt,P) = −17 Hz, ^4J(P,P) = 30 Hz, **10c**).

From this solution, the solvent was removed under vacuo, and the crude product was purified by preparative centrifugal thin layer chromatography using at first *n*-pentane/diethyl ether (5/1), then chloroform/diethyl ether (2/1), and finally chloroform/acetone/methanol (3/3/1). From the last fraction, the solvent was removed under vacuo. The yellow oil was investigated by NMR spectroscopy. Yield: 43 mg (48%). ^{1}H NMR (200 MHz, $CDCl_3$): δ 0.87 (t, ^3J(H,H) = 7.47 Hz, 27H, CH_3), 1.39 (s(br), 36H, CH_2), 1.69 (s(br), 18H, CH_2), 2.36 (s+m, ^3J(Pt,H) = 47.3 Hz, 9H, SCH_3). ^{13}C NMR (50 MHz, $CDCl_3$) δ 13.7 (s, *C*H_3), 21.1 (s(br), S*C*H_3), 24.2 (′t′, N = 13.7 Hz, γ-*C*H_2), 26.7 (m, β-*C*H_2), 27.7 (m(br), α-*C*H_2). ^{31}P NMR (81 MHz, $CDCl_3$): δ −7.2 (m, ^1J(Pt,P) = 3930 Hz, ^1J(Pt,Pt) = 1855 Hz, ^2J(Pt,P) = 65 Hz, ^3J(P,P) = 71 Hz).

Reaction of 4b with PBu_3. To a solution of **4b** (200 mg, 0.123 mmol) in methylene chloride (5 mL) was added PBu_3 (75 mg, 0.37 mmol) at −70 °C. Directly after the addition of the phosphine, a dark-red solution was formed. After warming up to room temperature, preparative centrifugal thin layer chromatography using at first *n*-pentane/ether (5/1), then chloroform/ether (2/1), and finally chloroform/acetone/methanol (3/3/1) was performed. From the last fraction, the solvent was removed under vacuo, and the yellow oil was investigated by NMR spectroscopy. Yield: 110 mg (62%). ^{1}H NMR (200 MHz, CD_2Cl_2): δ 0.72 (m, 36H, CH_3 (SEt), CH_3 (Bu)), 1.05 (m, 9H, SCH_2), 1.28(m, 36H, β-, γ-CH_2), 2.08 (m, 18H, α-CH_2). ^{13}C NMR (50 MHz, CD_2Cl_2): δ 13.6 (s, *C*H_3), 21.8 (s+d, ^3J(Pt,C) = 49.1 Hz, *C*H_3 (SEt)), 24.3 (m, γ-*C*H_2), 26.6 (m, β-*C*H_2), 29.0 (m, α-*C*H_2), 33.1 (s(br), *C*H_2 (SEt)). ^{31}P NMR (81 MHz, CD_2Cl_2): δ −8.1 (m, ^1J(Pt,P) = 3942 Hz, ^1J(Pt,Pt) = 1810 Hz, ^2J(Pt,P) = 67 Hz, ^3J(P,P) = 71 Hz).

3.3.2. Reactivity toward dppm. To a solution of **4** (0.13 mmol) in methylene chloride (5 mL) was added a solution of dppm (150 mg, 0.78 mmol) in methylene chloride (2 mL) dropwise with stirring at −70 °C. During the addition of the ligand, the color of the reaction mixture changed to dark-red. After warming up to room temperature, the color changed to light-yellow. The solvent was removed under vacuo, and the residue was washed with *n*-pentane/diethyl ether (3/1 mL). This residue was purified by preparative centrifugal thin layer chromatography using at first using *n*-pentane/diethyl ether (5/1), then chloroform/acetone (2/1), and finally chloroform/acetone/methanol (6/6/1) to elute the phosphines, [(PtL)$_2$(μ-SMe)(μ-dppm)]Cl (**12**), and ([Pt(SMe)$_2$(dppm)] (**13**), respectively. From the last two fractions the solvent was removed. The yellow platinum(I) complexes **12a**/**12b** and the white platinum(II) complex **13** were crystallized from chloroform/*n*-pentane (2/7 mL) solutions. After 2 days, the air-stable crystals were filtered off, washed with *n*-pentane (10 mL), and dried in vacuo. The dinuclear platinum(I) complex **12c** was obtained after chromatographic purification as a yellow oil.

[{Pt(PPh_3)}$_2$(μ-SMe)(μ-dppm)]Cl (12a). Yield: 90 mg (73%). T_{dec}: 161 °C. Found: C, 51.18; H, 4.09. $C_{62}H_{55}P_4SClPt_2\cdot 0.5CH_2Cl_2$ (1422.17) requires C, 52.74; H, 3.97. ^{1}H NMR (200 MHz, $CDCl_3$): δ 1.31 (′t′+d′t′, ^3J(Pt,H) = 41.5 Hz, N = 10.79 Hz, 3H, CH_3), 2.30 (s(br), 2H, CH_2), 7.13 (m(br), 50H, Ph). ^{13}C NMR (50 MHz, $CDCl_3$): δ 22.1 (′t′+d′t′, N = 3.9 Hz, ^2J(Pt,C) = 19.8 Hz, S*C*H_3), 62.3 (s(br), *C*H_2), 128.6 (m(br), 130.6 (s(br), 130.9 (s(br), 133.2 (m(br), 133.6 (m(br). ^{31}P NMR (81 MHz, $CDCl_3$): δ −3.9 (m,^1J(Pt,Pt) = 2770 Hz,^1J(Pt,P) = 3880 Hz,^2J(Pt,P) = −90 Hz, ^2J(P,P) = 40 Hz, ^2J(P,PPh_3) = 10 Hz, ^3J(P,PPh_3) = −20 Hz, *P*(dppm)), 21.9 (m, ^1J(Pt,P) = 3010 Hz, ^2J(Pt,P) = 170 Hz, ^3J(P,P) = 160 Hz, *P*Ph_3). ^{195}Pt NMR (107 MHz, $CDCl_3$): −5020 (m). IR: ν 3048(w), 2978(w), 1630(s), 1584(s),1478(m), 1433-(s), 1306(w), 1261(w), 1183(w), 1095(s), 997(w), 740(w), 691(s), 525-(s), 507(s), 486(s) cm^{-1}.

[{Pt{P(4-FC_6H_4)$_3$}}$_2$(μ-SMe)(μ-dppm)]Cl (12b). Yield: 84 mg (65%). T_{dec}: 182 °C. ^{1}H NMR (200 MHz, $CDCl_3$): δ 1.63 (′t′+d′t′, ^3J(Pt,H) = 41.5 Hz, N = 11.62 Hz, 3H, CH_3), 2.28 (s(br), 2H, CH_2), 6.93 (m(br), 18H, Ph), 7.20 (m(br), 26H, Ph). ^{13}C NMR (100 MHz, $CDCl_3$): δ 22.9 (′t′+d′t′, N = 3.9 Hz, ^2J(Pt,C) = 19.2 Hz, S*C*H_3), 60.0 (s(br), *C*H_2), 115.9 (m, *m*-*C*H), 128.2 (′t′, N = 10.3 Hz), 128.4 (m), 130.4 (s(br), 133.1 (m), 135.7 (m), 164.1 (d, ^1J(C,F) = 253.4 Hz, *C*F). ^{19}F NMR (188 MHz, $CDCl_3$): δ −109.18 (s(br), C*F*). ^{31}P NMR (81 MHz, $CDCl_3$): δ −3.7 (m, ^1J(Pt,Pt) = 2850 Hz, ^1J(Pt,P) = 3875 Hz, ^2J(Pt,P) = −85 Hz, ^2J(P,P) = 30 Hz, ^2J(P,P(4-FC_6H_4)$_3$) = 13 Hz, ^3J(P, P(4-FC_6H_4)$_3$) = −16 Hz, *P*(dppm)), 19.9 (m, ^1J(Pt,P) = 3055 Hz, ^2J(Pt,P) = 188 Hz, ^3J(P,P) = 170 Hz, *P*(4-FC_6H_4)$_3$). IR: ν 3048-(w), 3013(w), 2914(w), 2851(w), 1622(w), 1585(s), 1493(s), 1434(m), 1392(w), 1302(w), 1224(m), 1159(s), 1095(s), 948(w), 829(m), 814-(m), 738(m), 692(m), 526(s) cm^{-1}.

[{Pt(PBu_3)}$_2$(μ-SMe)(μ-dppm)]Cl (12c). Yield: 77 mg (71%). ^{1}H NMR (400 MHz, $CDCl_3$): δ 0.76 (t, ^3J(H,H) = 7.06 Hz, 18H, CH_3), 1.73 (m, 24H, β-, γ-CH_2), 1.38 (m, 12H, α-CH_2), 2.27 (s(br), 2H, CH_2), 2.66 (′t′+d′t′, ^3J(Pt,H) = 43.6 Hz, N = 11.21 Hz, 3H, SCH_3), 7.26 (m(br), 20H, Ph). ^{13}C NMR (100 MHz, $CDCl_3$): δ 13.7 (s, *C*H_3), 23.9 (′t′+d′t′, N = 3.7 Hz,^2J(Pt,C) = 20.6 Hz, S*C*H_3), 24.2 (′t′, N = 13.3 Hz, γ-*C*H_2), 26.4 (′t′, N = 16.9 Hz, β-*C*H_2), 27.1 (′quin′, N = 51.6 Hz, α-*C*H_2), 63.9 (s(br), *C*H_2), 128.3 (m(br), 128.6 (′t′, N = 11.8 Hz), 131.2 (s(br), 133.0 (m(br). ^{31}P NMR (81 MHz, $CDCl_3$): δ −5.7 (m, ^1J(Pt,-Pt) = 2380 Hz, ^1J(Pt,P) = 3925 Hz, ^2J(Pt,P) = −86 Hz, ^2J(P,P) = 25 Hz, ^2J(P,PBu_3) = 10 Hz, ^3J(P,PBu_3) = −21 Hz, *P*(dppm)), 7.3 (m, ^1J(Pt,P) = 2948 Hz, ^2J(Pt,P) = 70 Hz, ^3J(P,P) = 150 Hz, *P*Bu_3).

[Pt(SMe)$_2$(dppm)] (13). Yield: 22 mg (75%). T_{dec}: 142 °C. ^{1}H NMR (200 MHz, $CDCl_3$): δ 2.19 (t+dt, ^3J(Pt,H) = 49.0 Hz, ^4J(P,H) = 5.0 Hz, 6H, CH_3), 4.28 (t+dt, ^2J(P,H) = 10.4 Hz, ^3J(Pt,H) = 44.2 Hz, 2H, CH_2), 7.42 (m, 12H, Ph), 7.83 (m, 8H, Ph). ^{13}C NMR (100 MHz, $CDCl_3$): δ 12.2 (t+dt, ^2J(Pt,C) = 22.0 Hz, ^3J(P,C) = 2.3 Hz, *C*H_3), 48.7 (t+dt, ^2J(Pt,C) = 36.7 Hz, ^1J(P,C) = 30.2 Hz, *C*H_2), 128.1 (′d′, N = 25.0 Hz), 128.5 (′d′, N = 6.9 Hz), 128.7 (s(br)), 129.0 (′t′, N = 5.6 Hz), 131.6 (s(br), 132.8 (′d′, N = 20.3 Hz), 133.3 (′t′, N = 6.1 Hz), 133.7 (′d′, N = 19.5 Hz). ^{31}P NMR (81 MHz, $CDCl_3$): δ −47.0 (s+d,^1J(Pt,P) = 2362 Hz). IR: ν 3046(w), 2914(w), 2358(m), 1479-(m), 1434(s), 1096(s), 743(m), 693(s), 528(s) cm^{-1}.

3.3.3. Reactivity toward Br_2 and I_2. To a solution of **4a** (200 mg, 0.13 mmol) in methylene chloride (5 mL) cooled down to −70 °C was slowly added a solution of the requisite halogen (0.13 mmol) in methylene chloride (5 mL) with rigorous stirring to avoid a local overdose. After each drop, the color of the mixture changed from yellow to brown and back to yellow. The solution was allowed to warm to room temperature, and the solvent was removed under vacuo. The

residue was purified by preparative centrifugal thin layer chromatography using chloroform/acetone/methanol (1/1/1) followed by recrystallization from methylene chloride/diethyl ether (5/2 mL) ([{PtBr(PPh$_3$)}$_2$(μ-SMe)$_2$] (**14a**)) or chloroform/diethyl ether solutions (5/2 mL) ([{PtI(PPh$_3$)}$_2$(μ-SMe)$_2$] (**14b**)). After 2 days, yellow, air-stable crystals were filtered off, washed with pentane (10 mL), and dried in vacuo.

[{PtBr(PPh$_3$)}$_2$(μ-SMe)$_2$] (14a). Yield: 130 mg (57%). T_{dec}: 194 °C. Found: C, 39.34; H, 3.52; S, 5.60. $C_{38}H_{36}P_2S_2Br_2Pt_2$ (1165.94) requires C, 39.11; H, 3.11; S, 5.48. ^{1}H NMR (200 MHz, CD_2Cl_2): δ 2.67 (t+dt, ^3J(Pt,H) = 33.2 Hz, ^4J(P,H) = 5.8 Hz, 3H, CH_3), 2.77 (t+dt, ^3J(Pt,H) = 34.9 Hz, ^4J(Pt,H) = 5.8 Hz, 3H, CH_3), 7.31 (m, 18H, Ph), 7.57 (m, 12H, Ph). ^{13}C NMR (50 MHz, CD_2Cl_2): δ 14.4 (s(br), *C*H$_3$), 19.1 (t, ^3J(P,C) = 16.8 Hz, *C*H$_3$), 128.3 (m, *m*-*C*H), 130.1 ('t', *N* = 116.7 Hz, *i*-*C*), 131.0 (s, *p*-*C*H), 134.7 (m, *o*-*C*H). ^{31}P NMR (81 MHz, CD_2Cl_2): δ 14.8 (s+m, ^1J(Pt,P) = 3298 Hz, ^2J(Pt,Pt) = 820 Hz, ^3J(Pt,P) −2 Hz, ^4J(P,P) = 7.0 Hz). IR: ν 3051(w), 2914(w), 2019(w), 1480(m), 1434(s), 1303(w), 1183(w), 1158(w), 1096(s), 1027(w), 998(w), 957(m), 744(s), 706(s), 692(s), 535(s), 513(s), 498(s) cm^{-1}.

[{PtI(PPh$_3$)}$_2$(μ-SMe)$_2$] (14b). Yield: 110 mg (45%). T_{dec}: 237 °C. Found: C, 36.22; H, 3.00; S, 4.91. $C_{38}H_{36}P_2S_2I_2Pt_2$ (1261.91) requires C, 36.14; H, 2.88; S, 4.91. ^{1}H NMR (200 MHz, CD_2Cl_2): δ 2.75 (t+dt, ^3J(Pt,H) = 36.4 Hz, ^4J(P,H) = 5.3 Hz, 3H, CH_3), 3.06 (t+dt, ^3J(Pt,H) = 38.4 Hz, ^4J(P,H) = 5.6 Hz, 3H, CH_3), 7.31 (m, 18H, Ph), 7.60 (m, 12H, Ph). ^{13}C NMR (50 MHz, CD_2Cl_2): δ 10.1 (s(br), *C*H$_3$), 19.0 (s(br), *C*H$_3$), 128.2 (m, *m*-*C*H), 130.9 (s, *p*-*C*), 131.3 (s(br), *i*-*C*), 134.8 (m, *o*-*C*H). ^{31}P NMR (81 MHz, CD_2Cl_2): δ 14.9 (s+m, ^1J(Pt,P) = 3239 Hz, ^2J(Pt,Pt) = 960 Hz, ^3J(Pt,P) −2 Hz, ^4J(P,P) = 8 Hz). IR: ν 3048(w), 2962(w), 1479(m), 1433(s), 1302(w), 1184(w), 1096(s), 997(w), 954(m), 744(m), 707(m), 691(s), 536(s), 511(s), 494(s) cm^{-1}.

3.3.4. Reactivity toward Chalcogens. A solution of **4a** (400 mg, 0.26 mmol) and sulfur (8 mg, 0.25 mmol) in benzene (7 mL) and a suspension of **4a** (400 mg, 0.26 mmol) and selenium (20 mg, 0.25 mmol) in benzene (7 mL), respectively, were heated up to 70 °C for 48 h. The color of the solution changed from yellow to brown. After cooling to room temperature, the solvent was removed under vacuum. The crude product was purified by preparative centrifugal thin layer chromatography using chloroform/acetone (1/1) followed by reprecipitation from chloroform/*n*-pentane solutions (2/5 mL). After 2 days, brown, air-stable powders were filtered, washed with pentane (10 mL), and dried in vacuo.

[{Pt(PPh$_3$)}$_3$(μ_3-S)(μ-SMe)$_3$]Cl (15a). Yield: 200 mg (47%). Found: C, 39.55; H, 3.67; S, 8.40. $C_{57}H_{54}S_4P_3ClPt_3\cdot CH_2Cl_2$ (1663.05) requires C, 41.85; H, 3.39; S, 7.69. ^{1}H NMR (200 MHz, $CDCl_3$): δ 2.10 (s+d,^3J(Pt,H) = 50.6 Hz, CH_3), 7.34 (m(br), 45H, Ph). ^{13}C NMR (100 MHz, $CDCl_3$): δ 20.5 (s(br), S*C*H$_3$), 128.6 (m, *m*-*C*H), 130.7 (m, *i*-*C*), 131.4 (s, *p*-*C*H), 133.6 (m, *o*-*C*H). ^{31}P NMR (81 MHz, $CDCl_3$): δ 8.7 (s+m, ^1J(Pt,P) = 3808 Hz, ^2J(Pt,Pt) = 480 Hz, ^3J(Pt,P) = −40 Hz, ^4J(P,P) = 6 Hz). ESI−MS: *m*/*z* (obsd/calcd for [{Pt(PPh$_3$)}$_3$(μ_3-S)(μ-SMe)$_3$]$^+$, %) 1540 (4/2), 1541 (12/11), 1542 (32/35), 1543 (76/71), 1544 (90/95), 1545 (100/100), 1546 (79/85), 1547 (62/65), 1548 (42/43), 1549 (23/26), 1550 (14/13), 1551 (6/7). IR: ν 3048(w), 2911(w), 2362(m), 2337(m), 1480(m), 1434(s), 1383(w), 1096(s), 747(m), 693(s), 534(s) cm^{-1}.

[{Pt(PPh$_3$)}$_3$(μ_3-Se)(μ-SMe)$_3$]Cl (15b). Yield: 160 mg (38%). T_{dec}: 152 °C. ^{1}H NMR (200 MHz, $CDCl_3$): δ 2.03 (s+d^3J(Pt,H) = 52.3 Hz, CH_3), 7.30 (m(br), 45H, Ph). ^{13}C NMR (100 MHz, $CDCl_3$): δ 22.3 (s(br), S*C*H$_3$), 128.6 (m, *m*-*C*H), 131.1 (m, *i*-*C*), 131.6 (s, *p*-*C*H), 133.8 (m, *o*-*C*H). ^{31}P NMR (81 MHz, $CDCl_3$): δ 5.9 (s+m, ^1J(Pt,P) = 3937 Hz, ^2J(Pt,Pt) = 400 Hz, ^3J(Pt,P) = −38 Hz, ^4J(P,P) = 5 Hz). ESI−MS: *m*/*z* (obsd/calcd for [{Pt(PPh$_3$)}$_3$(μ_3-Se)(μ-SMe)$_3$]$^+$, %) 1585 (2/3), 1586 (8/7), 1587 (19/17), 1588 (32/31), 1589 (60/51), 1590 (80/72), 1591 (92/92), 1592 (100/100), 1593 (90/95), 1594 (76/78), 1595 (56/59), 1596 (38/39), 1597 (22/24), 1598 (12/13), 1599 (6/7). IR: ν 3053(w), 2959(w), 2911(w), 1549(m), 1530(m), 1480(m), 1434(s), 1302(w), 1185(w), 1096(s), 998(w), 951(w), 748(m), 693(s), 534(s) cm^{-1}.

Table 4. Crystallographic and Data Collection Parameters for Complexes **4a**·4CHCl$_3$, **5c**·2CHCl$_3$, and **6**·Me$_2$CO

	4a·4CHCl$_3$	**5c**·2CHCl$_3$	**6**·Me$_2$CO
empirical formula	$C_{61}H_{58}Cl_{13}P_3Pt_3S_3$	$C_{50}H_{42}As_2Cl_8Pt_2S_2$	$C_{78}H_{72}ClOP_3Pt_3S_4$
M_r/g·mol^{-1}	2026.28	1530.58	1867.23
crystal size (mm)	0.61 × 0.32 × 0.10	0.22 × 0.18 × 0.16	0.22 × 0.15 × 0.15
crystal system	monoclinic	monoclinic	monoclinic
space group	$P2_1/n$	$P2_1/n$	$P2_1/n$
a/Å	14.483(2)	9.194(2)	28.655(7)
b/Å	26.555(5)	17.693(3)	15.065(2)
c/Å	18.961(3)	16.586(4)	18.692(5)
β/deg	95.12(2)	99.37(3)	88.07(3)
V/Å^3	7263(2)	2662.1(1)	2662.1(1)
Z	4	2	4
D_{calc}/g·cm^{-1}	1.853	1.909	1.538
μ(Mo K$_\alpha$)/mm^{-1}	6.431	6.997	5.427
F(000)	3888	1464	3632
θ range/deg	2.00−25.00	2.30−25.00	1.96−25.00
refln. collected	49731	18554	57386
refln. observed [$I > 2\sigma(I)$]	12113	4667	14180
refln. independent	9797	3799	10264
data/parameters/restraints	12113/748/0	4667/289/0	14180/813/0
goodness-of-fit on F^2	1.026	0.984	0.956
$R1$ ($\sum$)/$R1$ ($I > 2\sigma(I)$)	0.0410/0.0291	0.0395/0.0286	0.0679/0.0436
w$R2$ ($\sum$)/w$R2$ ($I > 2\sigma(I)$)	0.0747/0.0673	0.0709/0.0673	0.1231/0.1116
largest diff. peak and hole/e·Å^{-3}	1.379/−1.531	0.806/−0.827	2.469/−1.152
T_{min}/T_{max}	0.111/0.566	0.370/0.500	0.383/0.501

Table 5. Crystallographic and Data Collection Parameters for Complexes **12b**·2H$_2$O and **14b**·CHCl$_3$

	12a	**14a**·CH$_2$Cl$_2$
empirical formula	$C_{62}H_{55}ClP_4Pt_2S$	$C_{39}H_{38}Br_2Cl_2P_2Pt_2S_2$
M_r/g·mol^{-1}	1381.63	1253.65
crystal size (mm)	0.28 × 0.23 × 0.20	0.75 × 0.37 × 0.37
crystal system	monoclinic	triclinic
space group	$P2_1/n$	$P\bar{1}$
a/Å	11.293(1)	11.350(2)
b/Å	29.191(5)	13.561(3)
c/Å	16.471(2)	14.212(3)
α/deg	90.00	98.75(2)
β/deg	91.44(2)	112.40(2)
γ/deg	90.00	92.88(3)
V/Å^3	5428.1(1)	1984.6(7)
Z	4	2
D_{calc}/g·cm^{-1}	1.691	2.098
μ(Mo K$_\alpha$)/mm^{-1}	5.394	9.403
F(000)	2704	1188
θ range/deg	2.16−25.00	1.97−25.91
refln. collected	23191	15269
refln. observed [$I > 2\sigma(I)$]	9301	7082
refln. independent	7344	6397
data/parameters/restraints	9301/632/0	7082/443/0
goodness-of-fit on F^2	1.036	1.077
$R1$ ($\sum$)/$R1$ ($I > 2\sigma(I)$)	0.0593/0.0439	0.0478/0.0423
w$R2$ ($\sum$)/w$R2$ ($I > 2\sigma(I)$)	0.1223/0.1080	0.1218/0.1148
largest diff. peak and hole/e·Å^{-3}	1.185/−2.792	1.888/−3.218
T_{min}/T_{max}	0.335/0.444	0.031/0.113

3.4. X-ray Crystal Structure Determinations. Intensity data were collected on Stoe-IPDS and Stoe-IPDS-2 diffractometers using graphite monochromatized Mo K$_\alpha$ radiation (λ = 0.71073 Å) at 220(2) K (**4a**·4CHCl$_3$, **5c**·2CHCl$_3$, **6**·Me$_2$CO, **14b**·CHCl$_3$) and 153 K (**12b**·2H$_2$O), respectively. A summary of the crystallographic data, the data collection parameters, and the refinement parameters are given in Tables 4 and 5. Absorption corrections were applied numerically. The structures were solved by direct methods with SHELXS-97 and refined using full-matrix least-squares routines against F^2 with SHELXL-97.[36] All non-hydrogen

(36) Sheldrick, G. M. SHELXS-97, SHELXL-97, Programs for Crystal Structure Determination, University of Göttingen: Göttingen, 1990/1997.

atoms were refined with anisotropic displacement parameters. H atoms were included to the models in calculated positions using the riding model. Crystallographic data (excluding structure factors) for the structures reported in this paper have been deposited at the Cambridge Crystallographic Data Center (CCDC) as Supplementary Publication No. CCDC-635203 (**4a**·4$CHCl_3$), CCDC-635204 (**5c**·2$CHCl_3$), CCDC-635205 (**6**·Me_2CO), CCDC-635206 (**12b**·2H_2O), and CCDC-635207 (**14b**·$CHCl_3$). Copies of the data can be obtained free of charge on application to the CCDC, 12 Union Road, Cambridge, CB2 1EZ, U.K. (fax, +44−1223-336033; E-mail, deposit@ccdc.cam.ac.uk).

3.5. Computational Details. All DFT calculations were performed by employing the Gaussian98 program package[37] using the MPW1PW91[38] functional. A triple-ζ valence basis set was used for Pt with a polarization function added (TZVP) as provided by Ahlrichs and co-workers.[39] For its core orbitals, an effective core potential with consideration of relativistic effects has been used.[40] For all other atoms, a split-valence basis set with polarization functions (P, S atoms: 6-31G*) and without polarization functions (C, H atoms: 3-21G) were used. The appropriateness of the functional in combination with the basis sets and effective core potential used for reliable interpretation of the electron density and structural aspects has been demonstrated.[41] The AIM analysis as well as the visualization were performed using the program package AIMPAC as provided by Bader et al.[42] All systems have been optimized in C_3 symmetry. The resulting geometries were characterized as equilibrium structures by the analysis of the force constants of normal vibrations.

Acknowledgment. Financial support from the Deutsche Forschungsgemeinschaft and gifts of chemicals from Merck (Darmstadt) are gratefully acknowledged.

Supporting Information Available: Energies and Cartesian coordinates of atom positions of the calculated cations [{$Pt(PPh_3)$}$_3$(μ-$SMe)_3$]$^+$ (**4a′**) and [{$Pt(PPh_3)$}$_3$(μ_3-S)(μ-$SMe)_3$]$^+$ (**15a′**). Crystallographic information files (cif) of the structures of [{$Pt(PPh_3)$}$_3$(μ-$SMe)_3$]Cl·4$CHCl_3$ (**4a**·4$CHCl_3$), [{$PtCl(AsPh_3)$}$_2$(μ-$SPh)_2$]·2$CHCl_3$ (**5c**·2$CHCl_3$), [{$Pt(PPh_3)$}$_3$(μ_3-S)(μ-$SBn)_3$]Cl·Me_2CO (**6**·Me_2CO), [{$Pt(PPh_3)$}$_2$(μ-SMe)(μ-dppm)]Cl (**12a**), and [{$PtBr(PPh_3)$}$_2$(μ-$SMe)_2$]·CH_2Cl_2 (**14a**·CH_2Cl_2).

JA068476R

(37) Frisch, M. J.; et al. *Gaussian98*, revision A.9; Gaussian Inc.: Pittsburgh, PA, 1998.
(38) Adamo, C.; Barone, V. *Chem. Phys. Lett.* **1997**, *274*, 242.
(39) Schaefer, A.; Huber, C.; Ahlrichs, R. *J. Chem. Phys.* **1994**, *100(8)*, 5829.
(40) Andrae, D.; Haeussermann, U.; Dolg, M.; Stoll, H.; Preuss, H. *Theor. Chim. Acta* **1990**, *77*, 123.
(41) Schwieger, S.; Wagner, C.; Bruhn, C.; Schmidt, H.; Steinborn, D. *Z. Allg. Anorg. Chem.* **2005**, *631*, 2696.
(42) http://www.chemistry.mcmaster.ca/aimpac/, 2000. The program was slightly changed to allow the appropriate number of basis functions.